

# First year of operation of SPIDER, prototype source of ITER neutral beam injectors

G. Serianni on behalf of NBTF team and  
contributing staff of ITER-IO, F4E, INDA, QST, NIFS, IPP and other European institutions

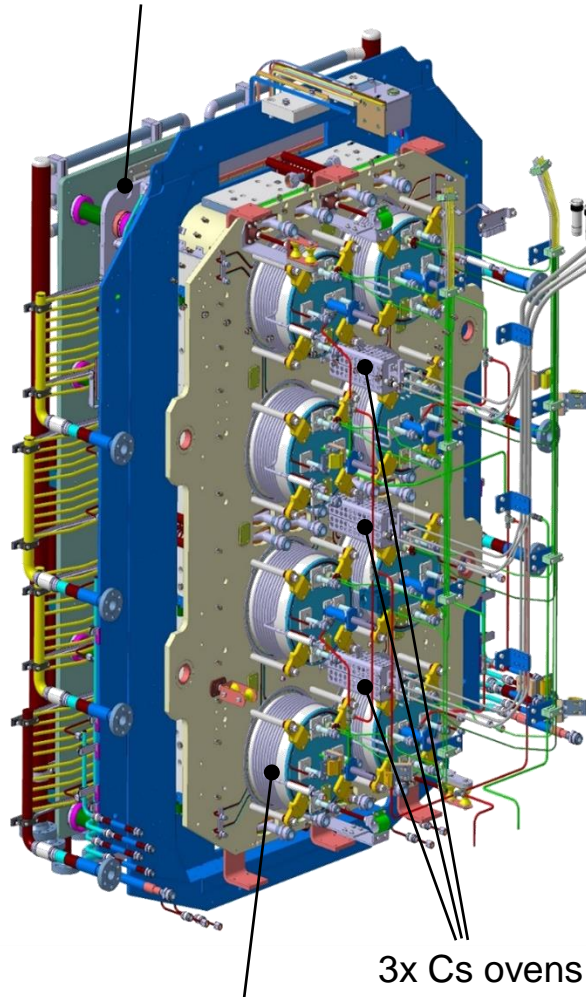
Consorzio RFX, Padova, Italy



- Few physics issues of neutral beams
- Main SPIDER components
- First operations of SPIDER, ion source of ITER Neutral Beam Injectors
  - First characterisation of beam

# SPIDER: full scale prototype of HNB/DNB source

Extractor and accelerator



8x RF drivers

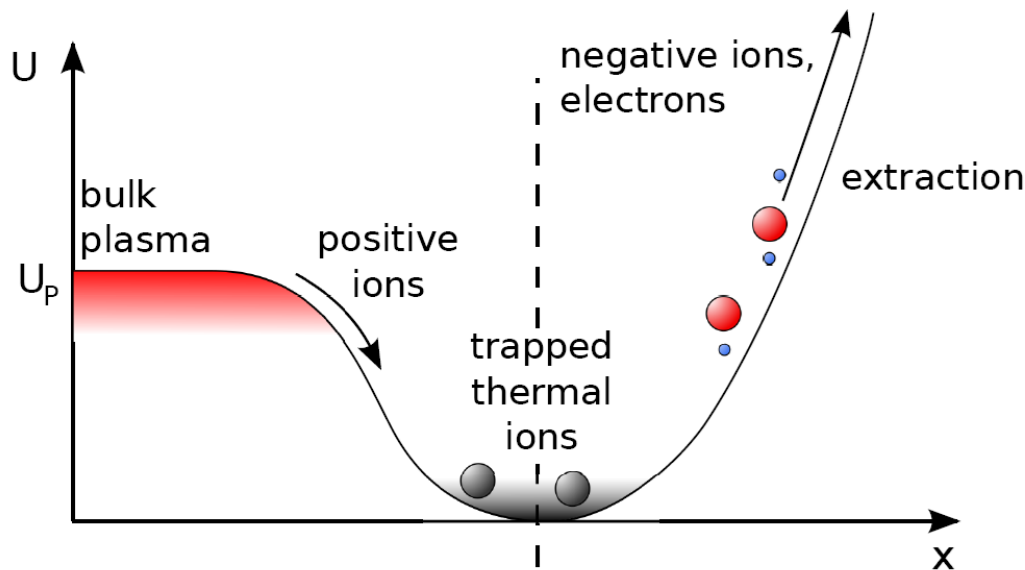
3x Cs ovens

- Optimisation of production of negative ions in terms of:

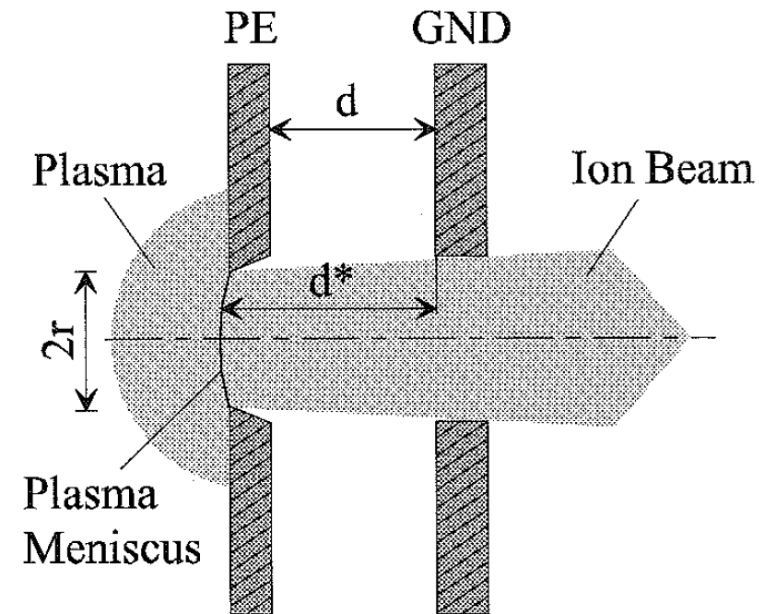
- Density
- Uniformity
- Stability
- Co-extracted electrons

	Unit	H	D
Beam energy	keV	100	100
Maximum Beam Source pressure	Pa	<0.3	<0.3
Uniformity	%	±10	±10
Extracted current density	A/m <sup>2</sup>	>355	>285
Beam on time	s	3600	3600
Co-extracted electron fraction (e <sup>-</sup> /H <sup>-</sup> ) and (e <sup>-</sup> /D <sup>-</sup> )		<0.5	<1

- Boundary/interface between (source) plasma & beam (accelerator)
  - Debye sheath, trapping positive ions, allowing extraction of electrons and H<sup>-</sup>
- Co-extracted electrons
- Meniscus curvature helps beam focussing



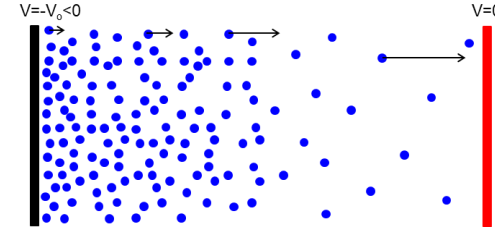
T. Kalvas, CERN Accelerator School 2012



I. G. Brown, The Physics and Technology of Ion Sources, Wiley

# Perveance

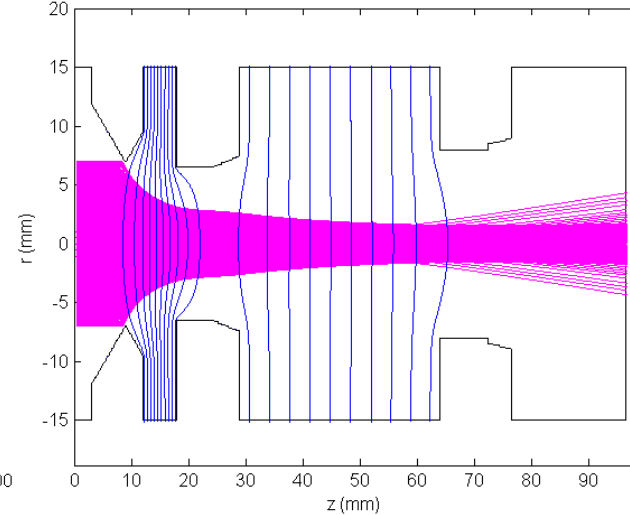
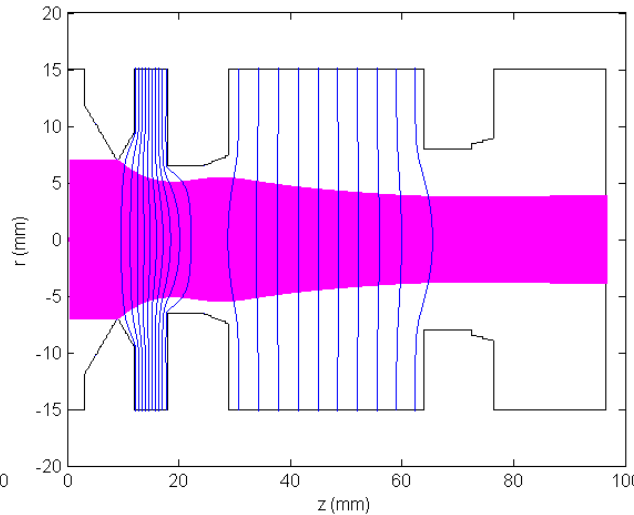
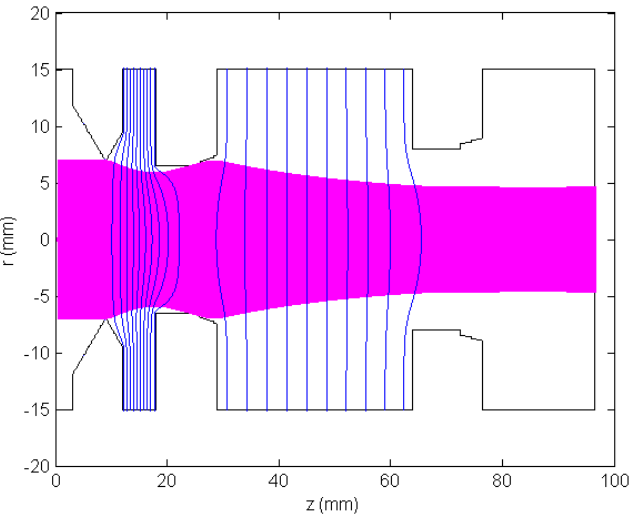
- From Child-Langmuir law: 
$$P = \frac{I}{V_0^{3/2}} = \frac{4}{9} \epsilon_0 \sqrt{\frac{2Ze}{m}} \frac{\pi r_a^2}{d^2}$$



461A/m<sup>2</sup>

355A/m<sup>2</sup>

177A/m<sup>2</sup>



Over-perveant beam:  
increased divergence!

If too large current density,  
particles repel each other

Optimal perveance

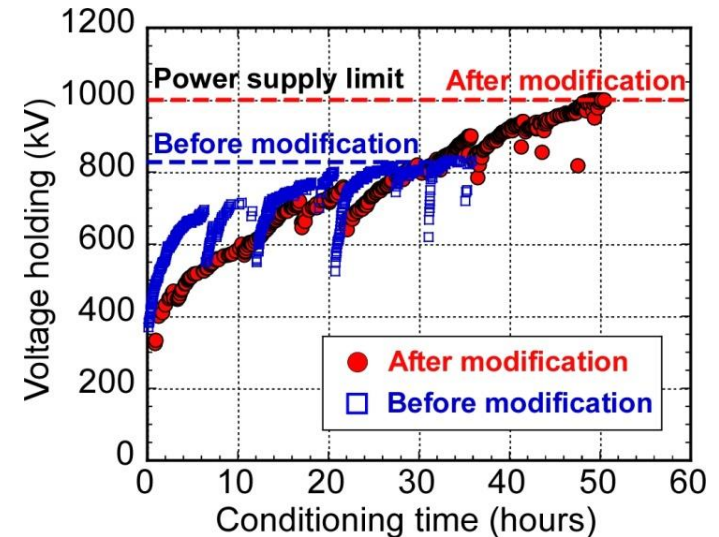
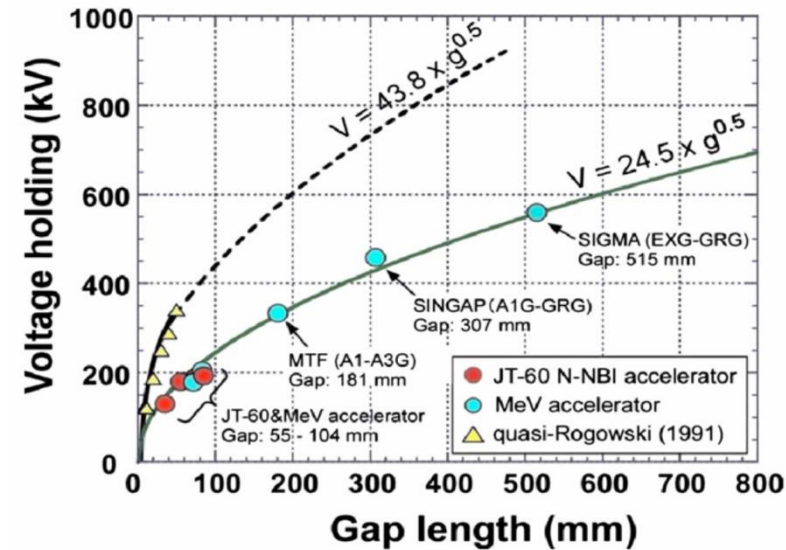
Under-perveant beam:  
increased divergence!

If too few particles, trajectories  
are squeezed by electric field

- Acceleration to 1MeV
  - Voltage holding can be an issue in multi-aperture accelerators (dashed line: parallel planar electrodes)
- Breakdown voltage  $\sim(\text{gap length})^{1/2}$

Brown, The Physics and Technology of Ion Sources, Wiley

- Accelerator conditioning required



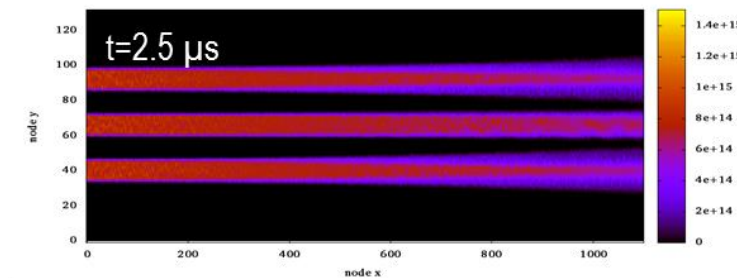
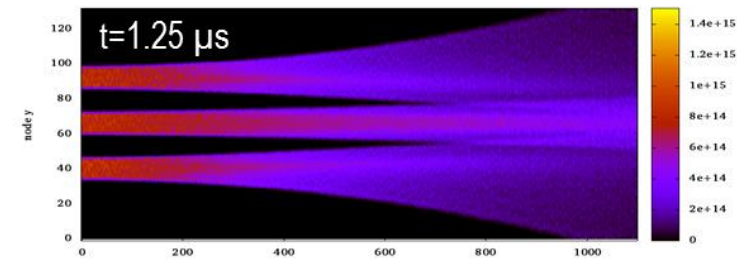
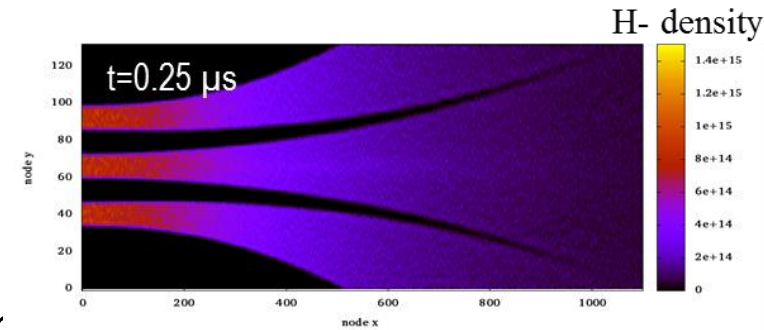
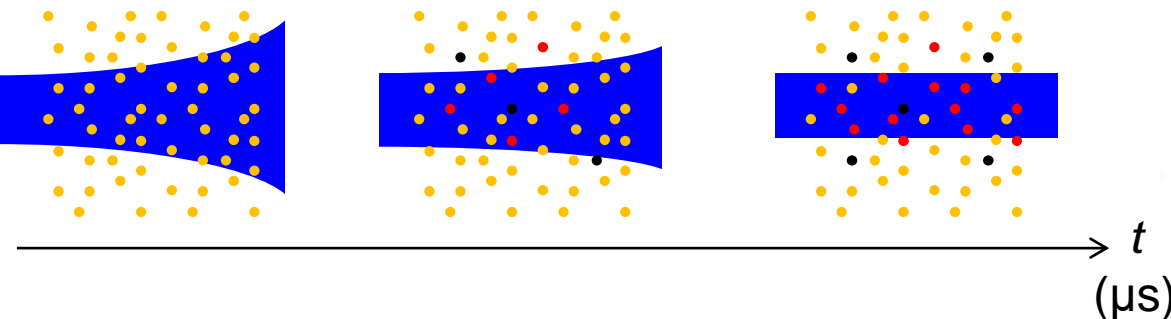


- Ionisation of background gas:

- $\underline{H}^0 + H_2 \rightarrow \underline{H}^0 + H_2^+ + e$
- Positive particle trapped in beam potential
- Negative particles (electrons) ejected from beam region

- Stationary equilibrium reached:

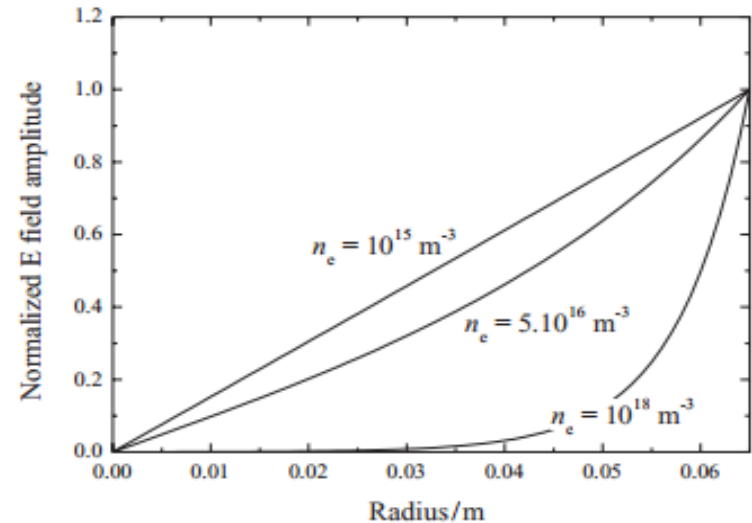
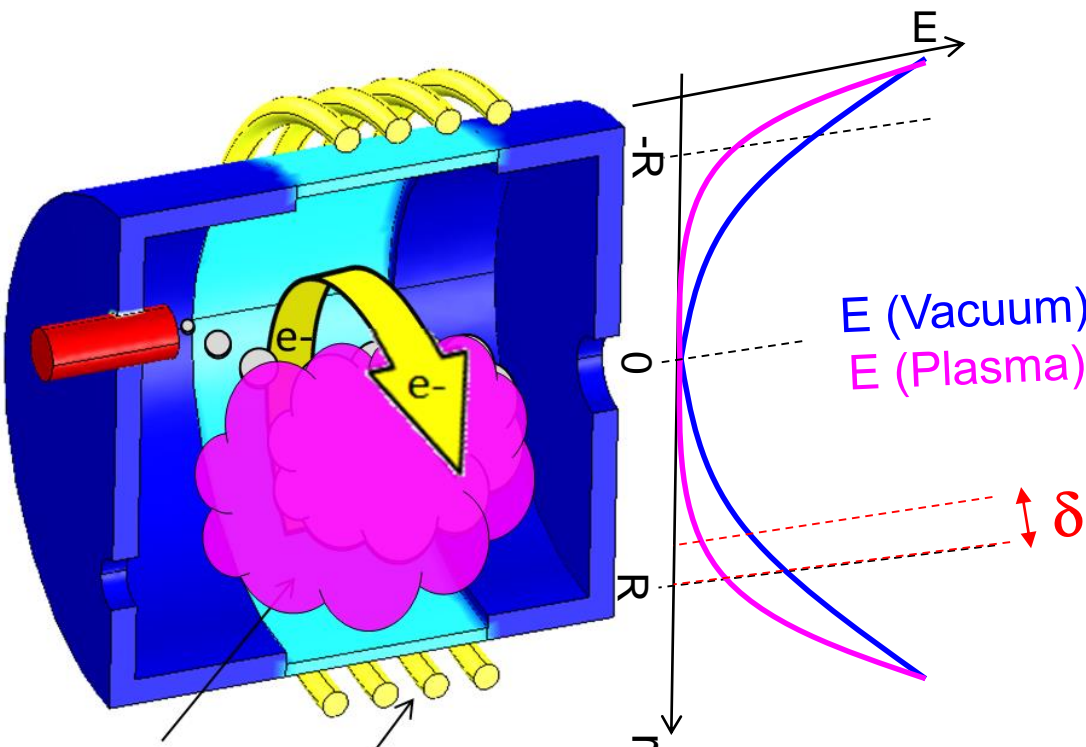
- Negative ion beams usually slightly overcompensated (unlike positive ion beams)



E. Sartori et al., Rev. Sci. Instrum. **87** (2016) 02B917

- Particle regime

- electric field forces electrons to oscillate
- when plasma is created it shields E field: i.e. wave is attenuated
- E field drops with typical length scale (skin depth)

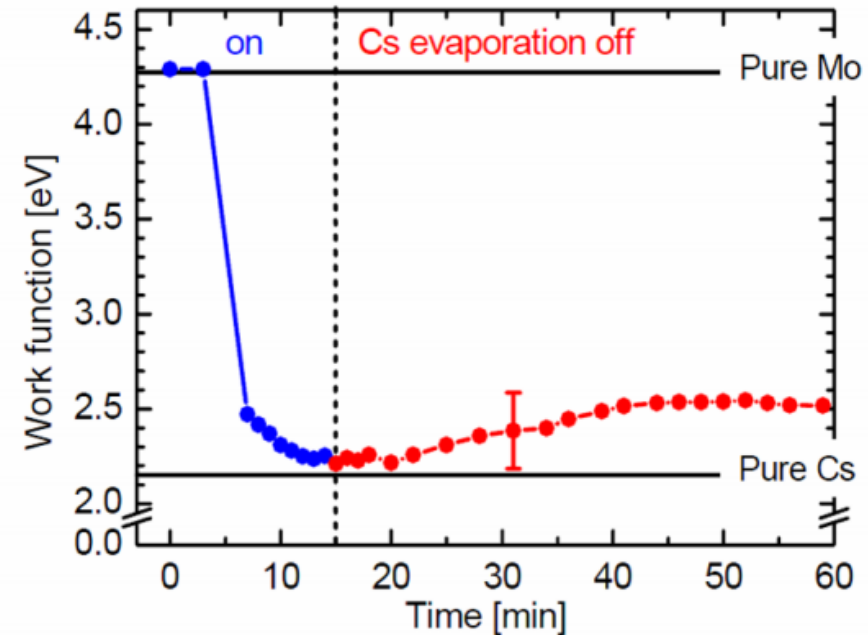


P. Chabert, Physics of RF Plasmas, Cambridge Univ. Press

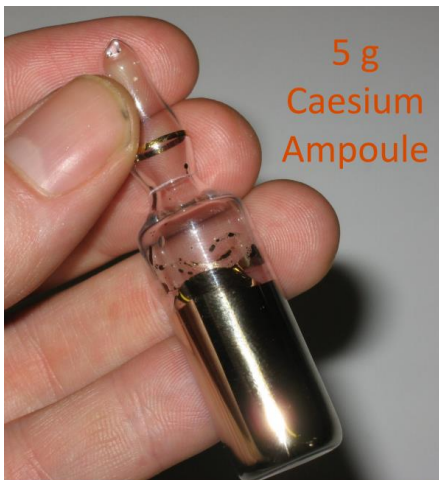


# On-going activities: caesium management and modelling

- Small quantity of caesium vapor increases negative ion yield
- The work function is reduced ( $\approx$ pure Cs)
- Source Conditioning needed
- Plasma grid temperature  $>140^\circ$
- Source body temperature  $35^\circ\text{C}$  to avoid trapping of Cs on the walls
- Many plasma pulses to distribute Cs



W. Kraus, CERN Accelerator School



## Surface Production:

- Need for Caesium
- Poor reproducibility
- Negative ion flux limited by space charge: plasma is needed

Vs.

## Volume Production:

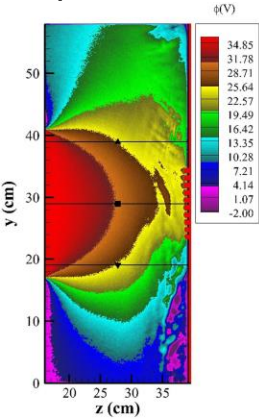
- ion currents  $< 30 \text{ A/m}^2$
- High co-extracted electron current

D. Faircloth, CERN  
Accelerator School

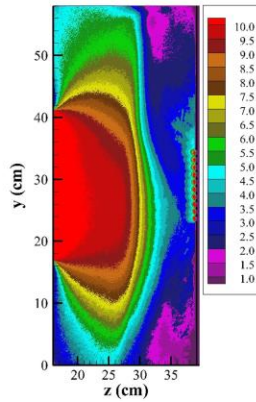
## Beam extraction modelling

### Plasma modelling

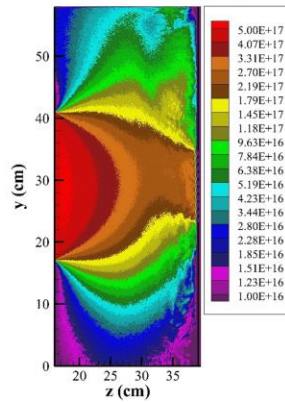
Electric potential



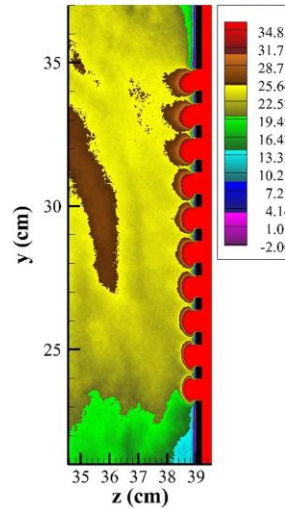
Electron temperature



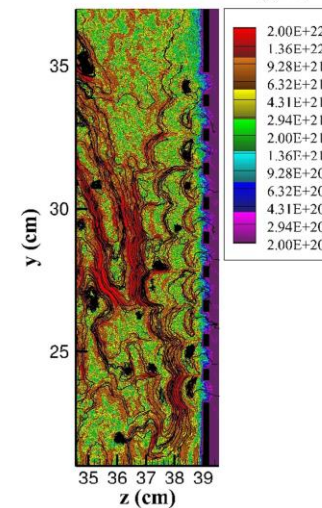
Electron density



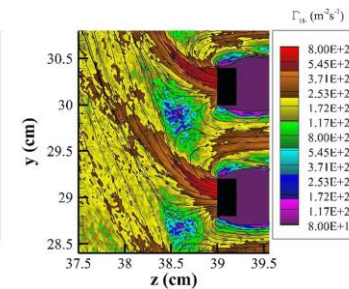
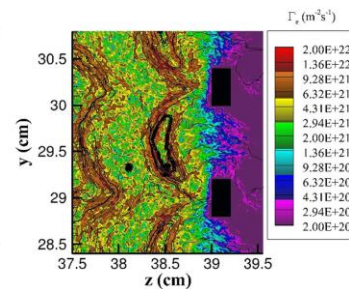
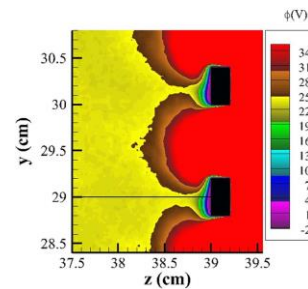
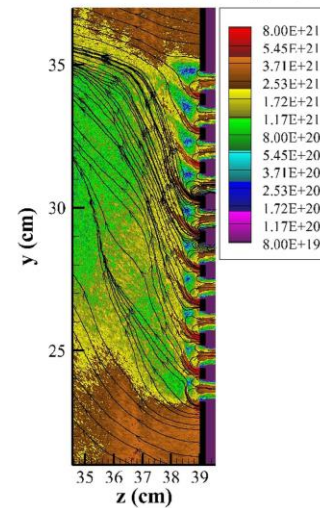
Electric potential



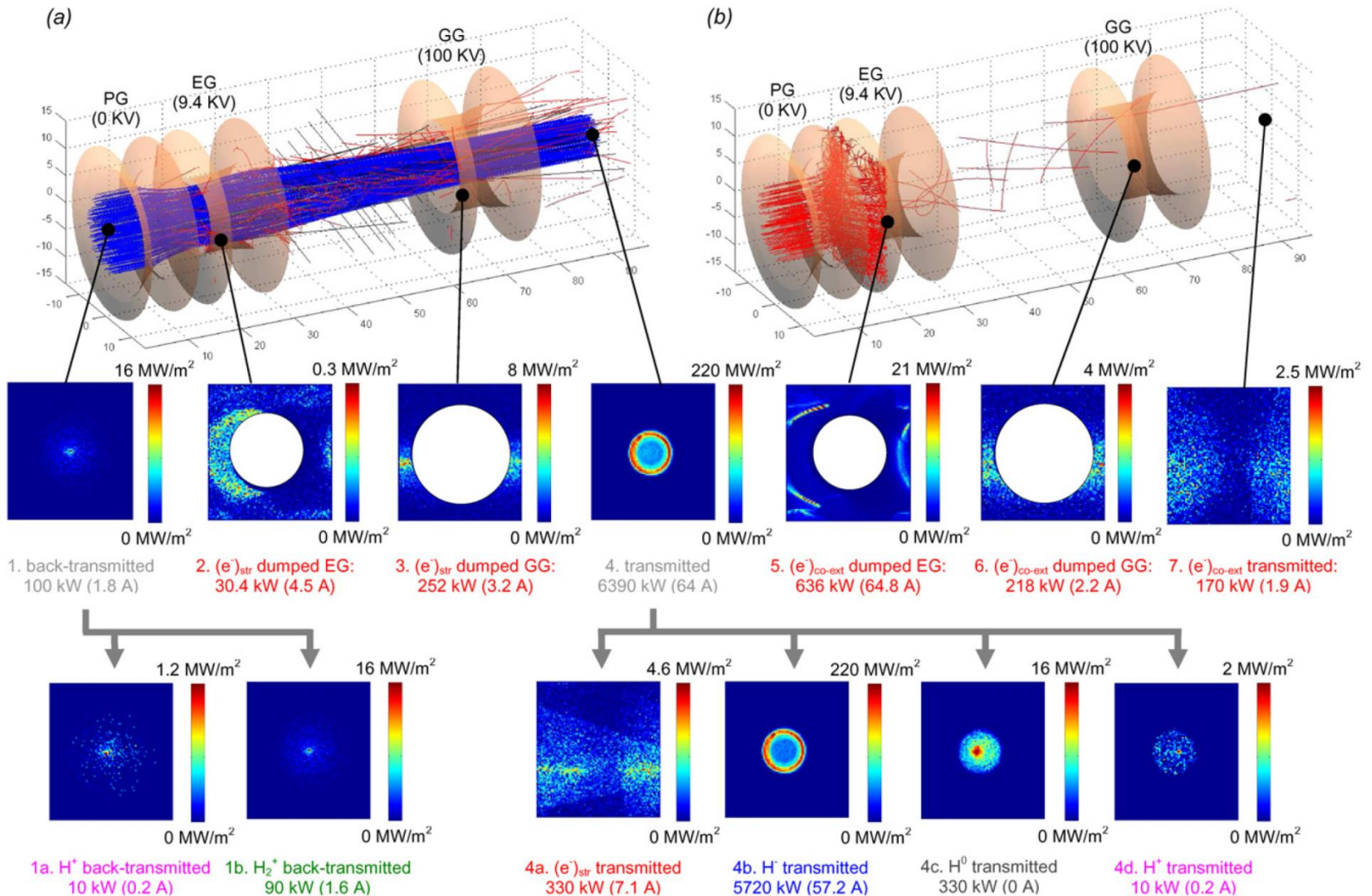
Electron flux



Negative ion flux



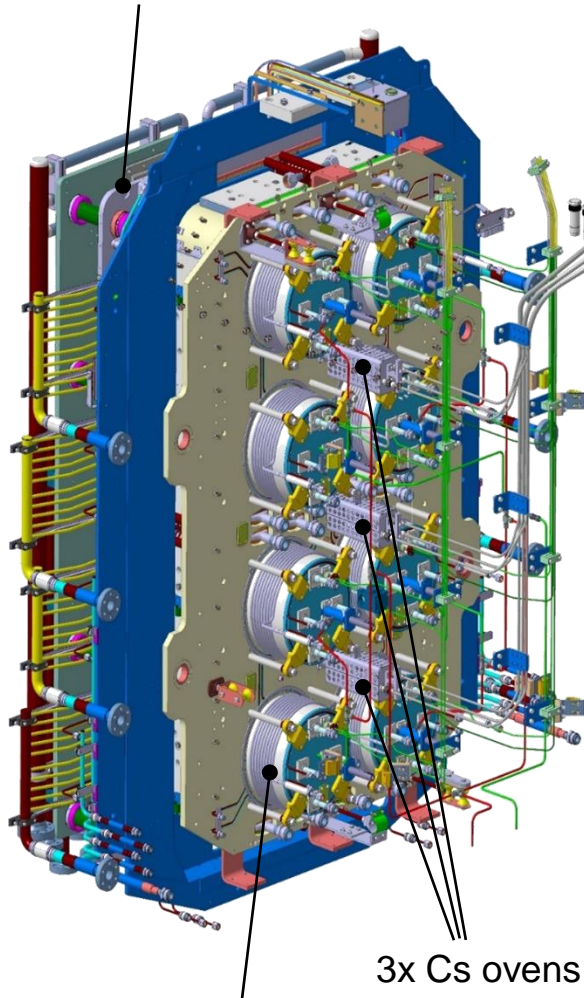
# On-going activities: beam transport modelling





# SPIDER: full scale prototype of HNB/DNB source

Extractor and accelerator



3x Cs ovens

8x RF drivers

- Optimisation of production of negative ions in terms of:

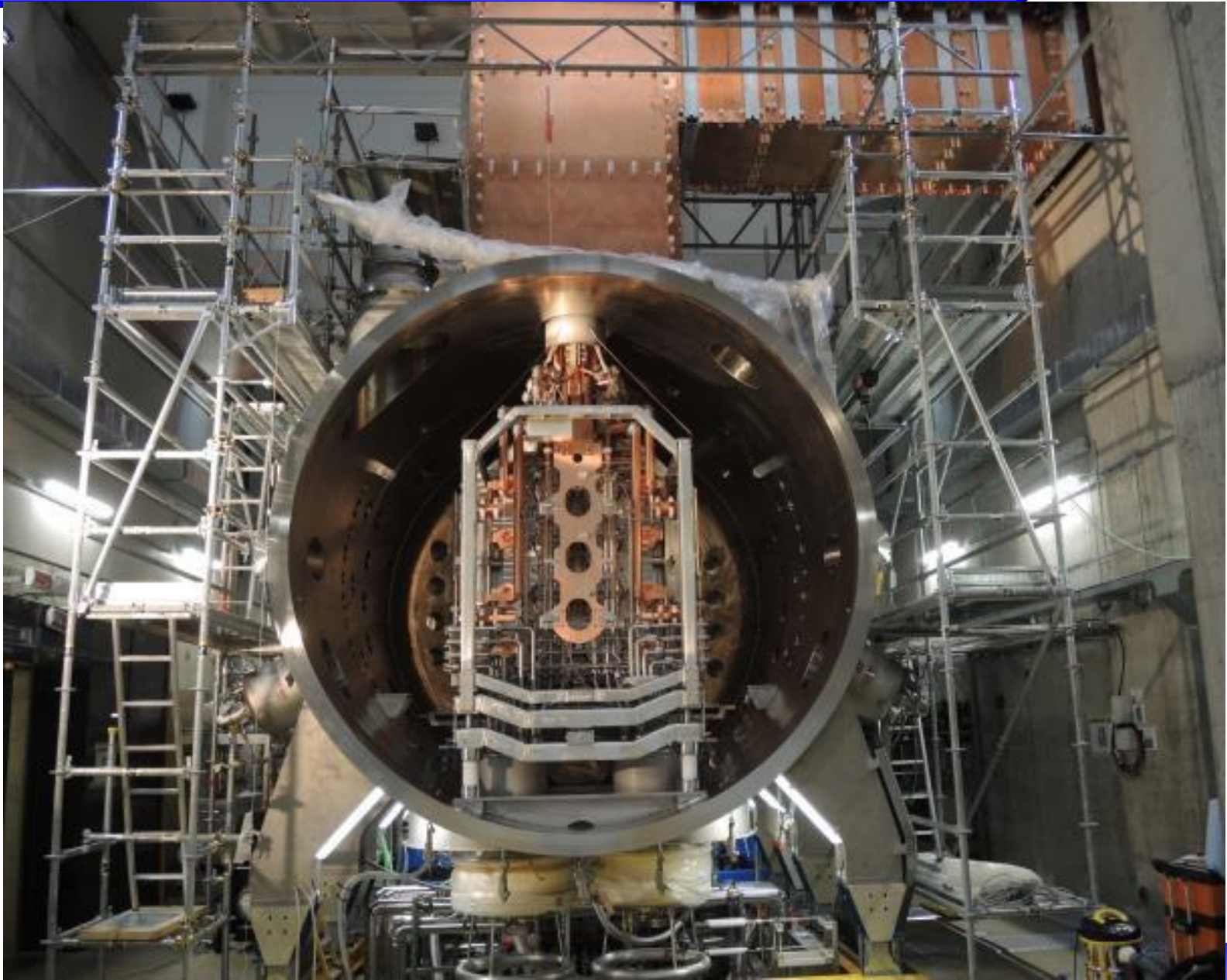
- Density
- Uniformity
- Stability
- Co-extracted electrons

	Unit	H	D
Beam energy	keV	100	100
Maximum Beam Source pressure	Pa	<0.3	<0.3
Uniformity	%	±10	±10
Extracted current density	A/m <sup>2</sup>	>355	>285
Beam on time	s	3600	3600
Co-extracted electron fraction (e <sup>-</sup> /H <sup>-</sup> ) and (e <sup>-</sup> /D <sup>-</sup> )		<0.5	<1

# SPIDER beam source inside vacuum vessel



**CONSORZIO RFX**  
Ricerca Formazione Innovazione

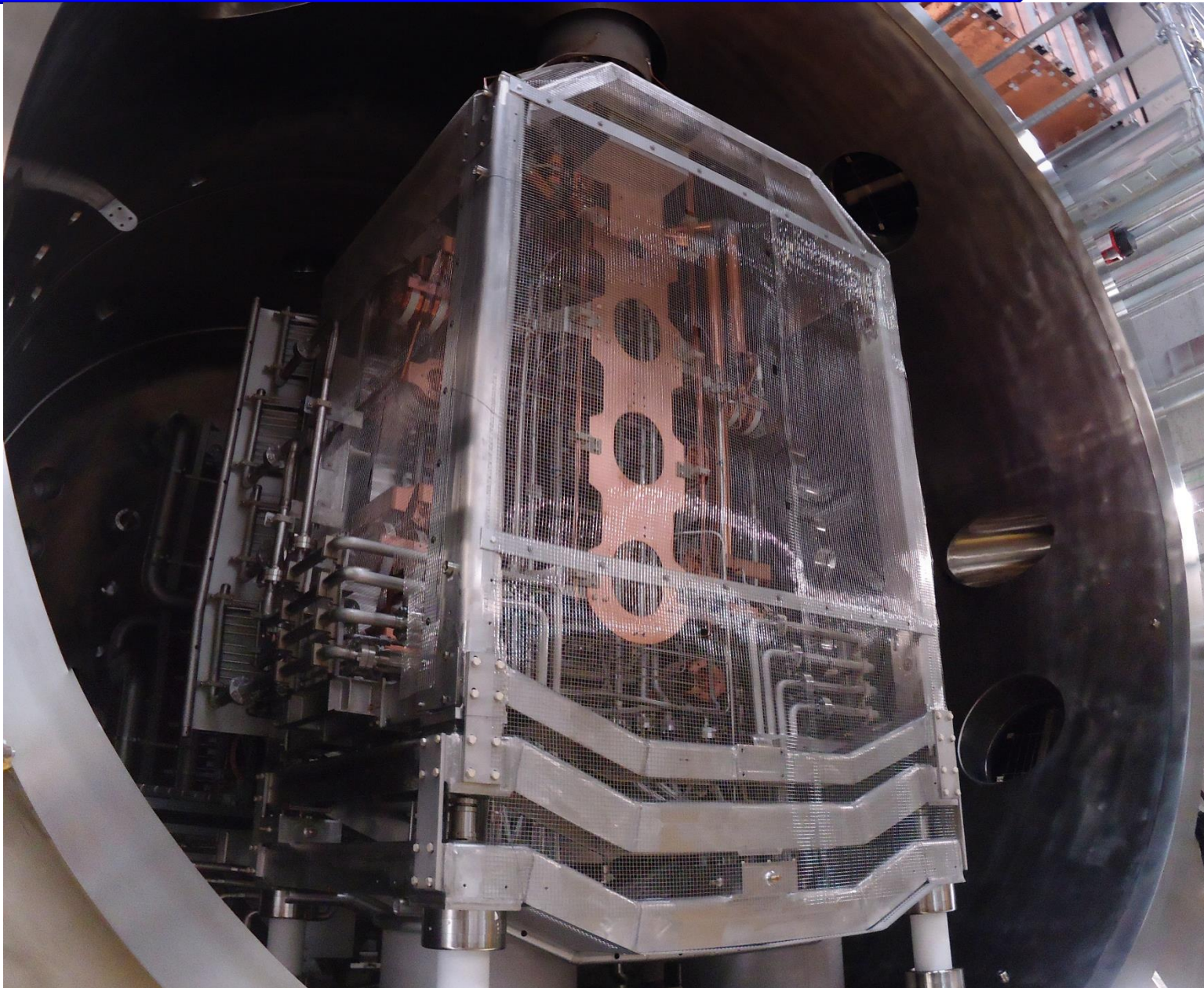




# SPIDER beam source inside vacuum vessel



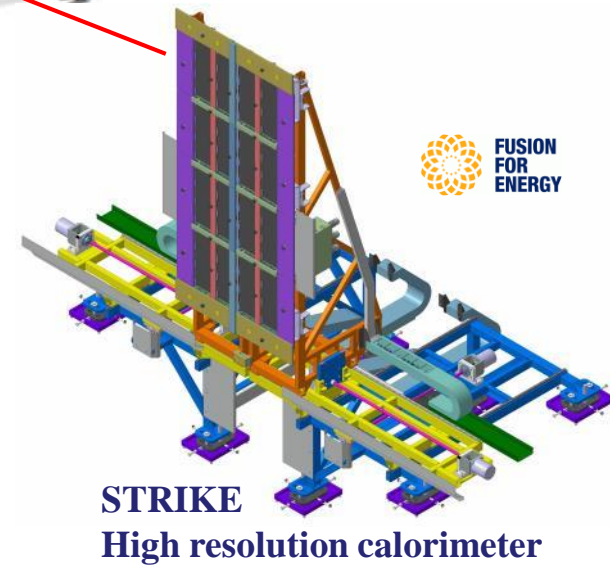
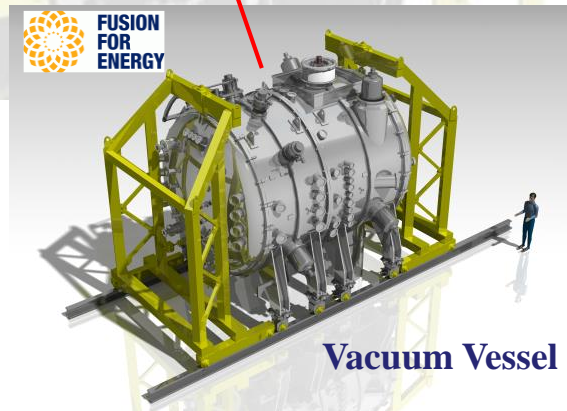
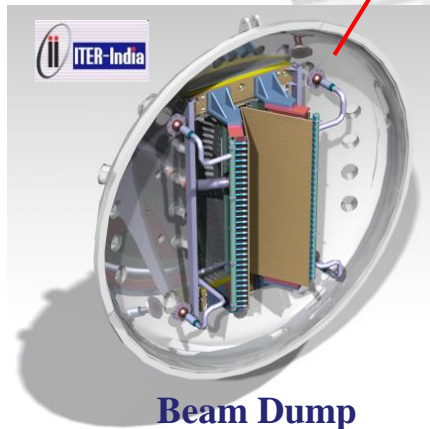
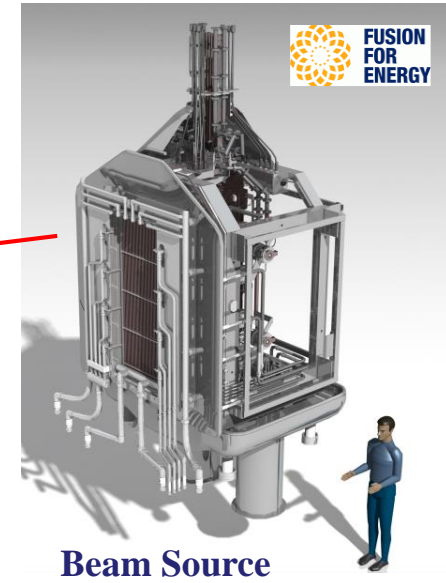
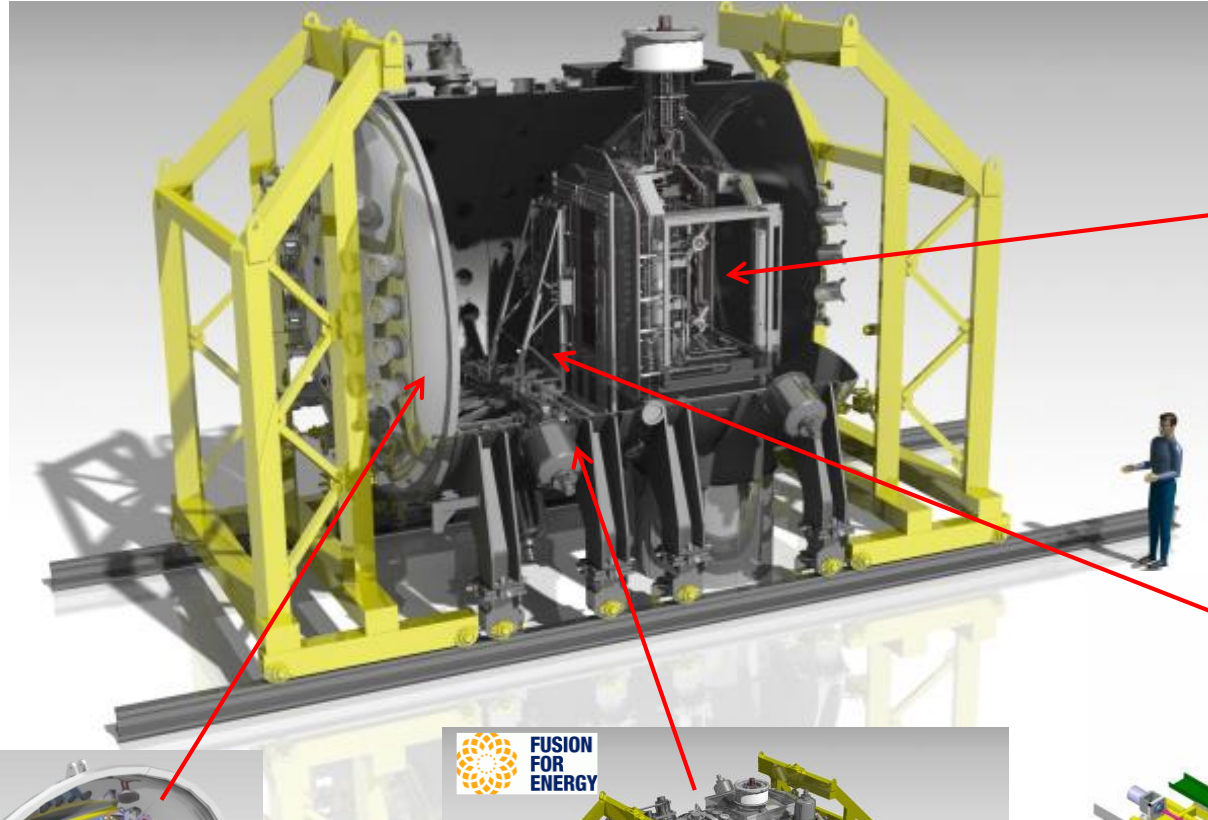
**CONSORZIO RFX**  
Ricerca Formazione Innovazione





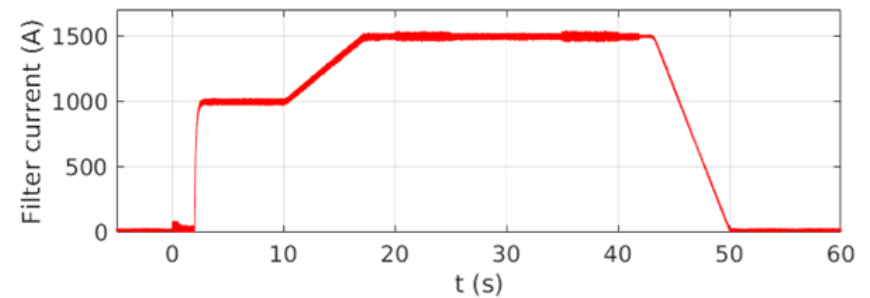
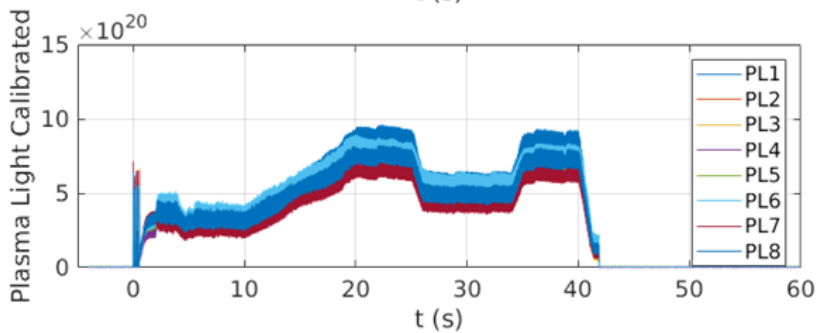
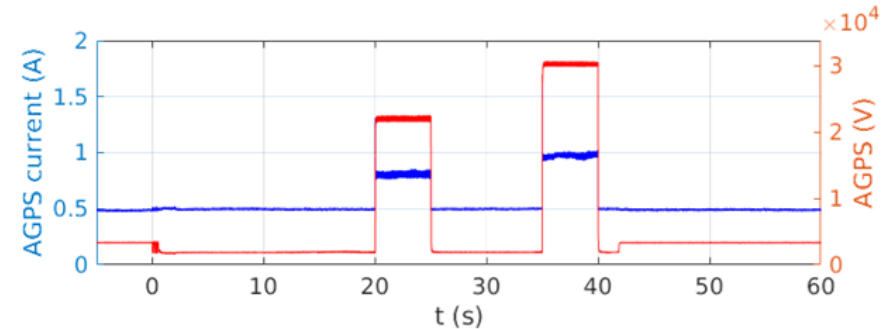
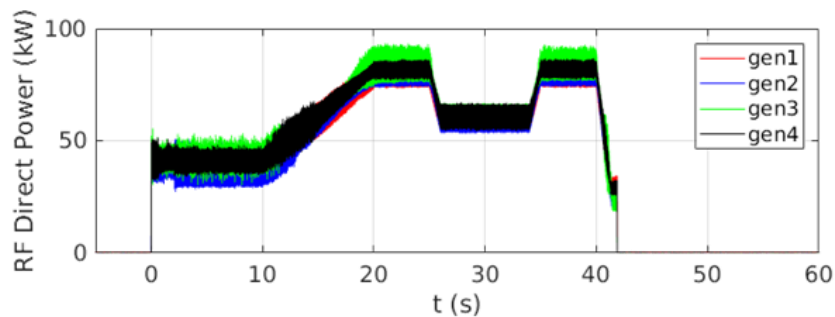
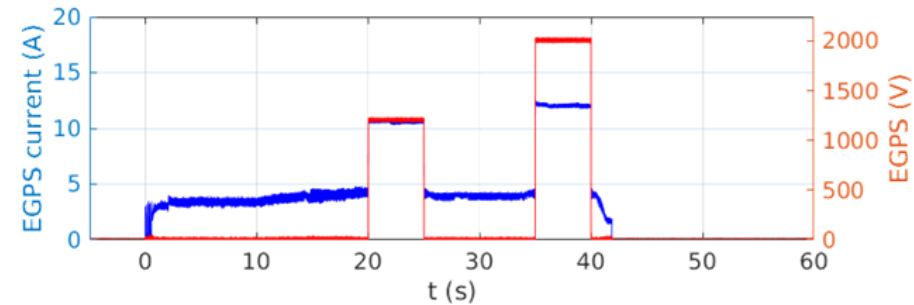
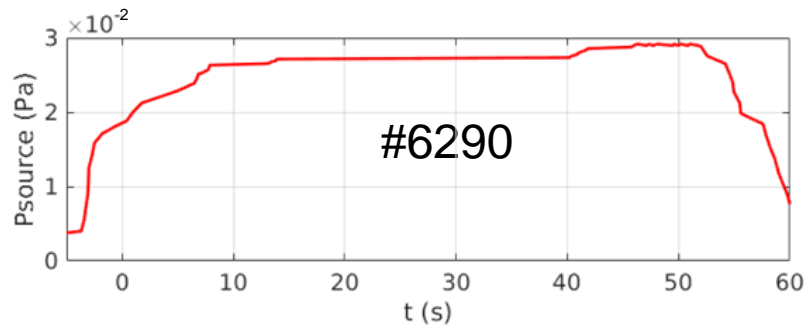
# SPIDER Components

## Vacuum-insulated beam source



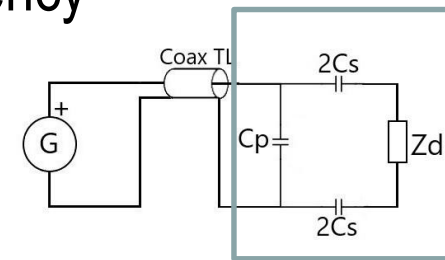
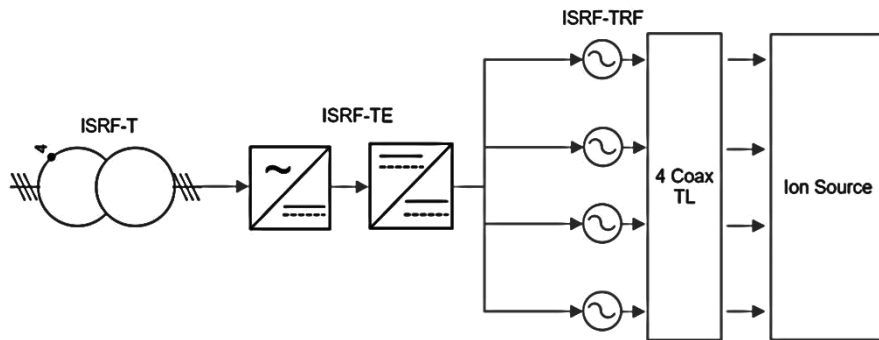
# Example of beam pulse

- Large flexibility of SPIDER control system

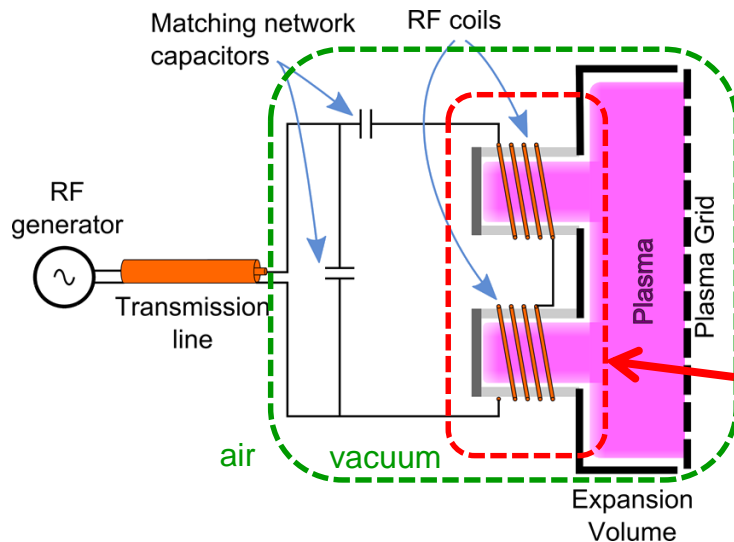


# The SPIDER RF system

- 4 RF generators (ISRF-TRF), transmission line (TL), ion source RF load
- Each RF generator: pair of **power tetrodes** in push-pull connection; **variable capacitor  $C_v$**  to tune operating frequency



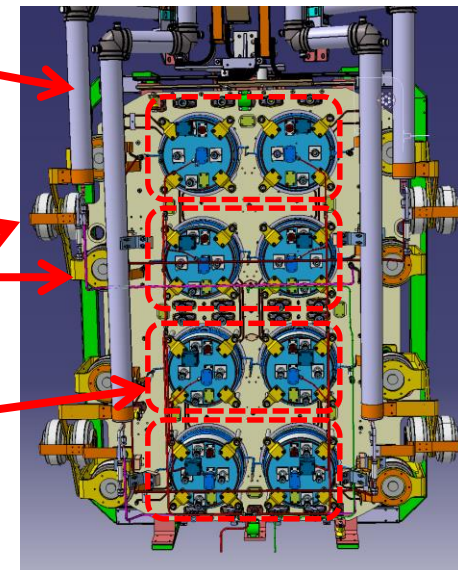
Ion source RF load



RF transmission lines connected to RF oscillators

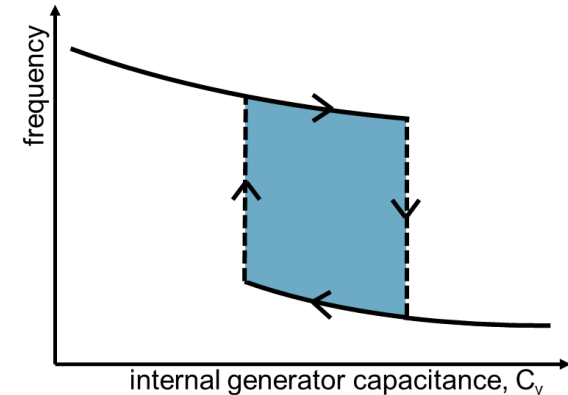
Matching network capacitors

Driver pairs

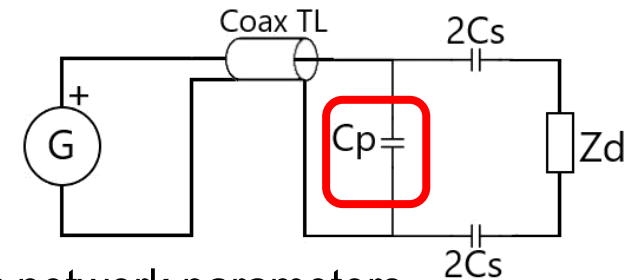


ISRF1  
ISRF3  
ISRF4  
ISRF2

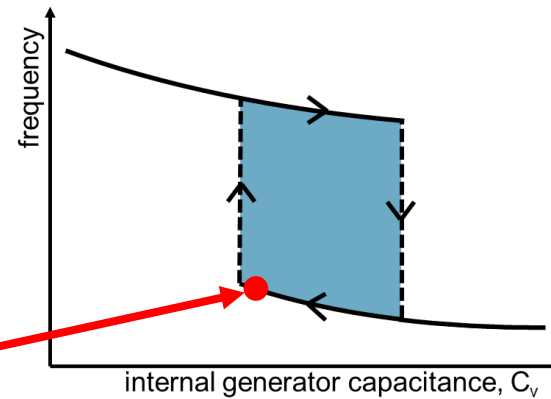
- **RF power limit** identified (80kW out of 200kW):
  - power transfer **depending** on equivalent load impedance
  - sudden **frequency flips** near impedance matching
    - RF power constrained, as observed in other facilities



- **Strategy:**
  - implementation of **feedforward control** of capacitor of RF generators ( $C_v$ )
  - development of **model** reproducing different behaviours of ISRF system to:
    - support SPIDER operation
    - analyse its performances
    - help in achieving nominal performances
  - **experimental campaign** to analyse different matching network parameters
    - different parallel capacitors in different circuits:  $C_p = 5 \text{ nF}$ ;  $6.5 \text{ nF}$ ;  $10 \text{ nF}$  (design value);  $15 \text{ nF}$



- Hysteresis depending on  $C_v$  observed and modelled
  - best  $C_v$  value near lower flip frequency

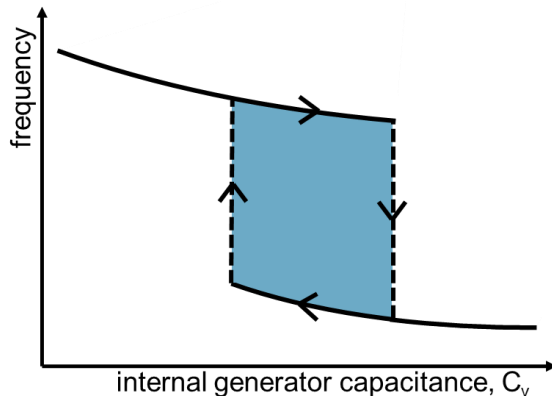
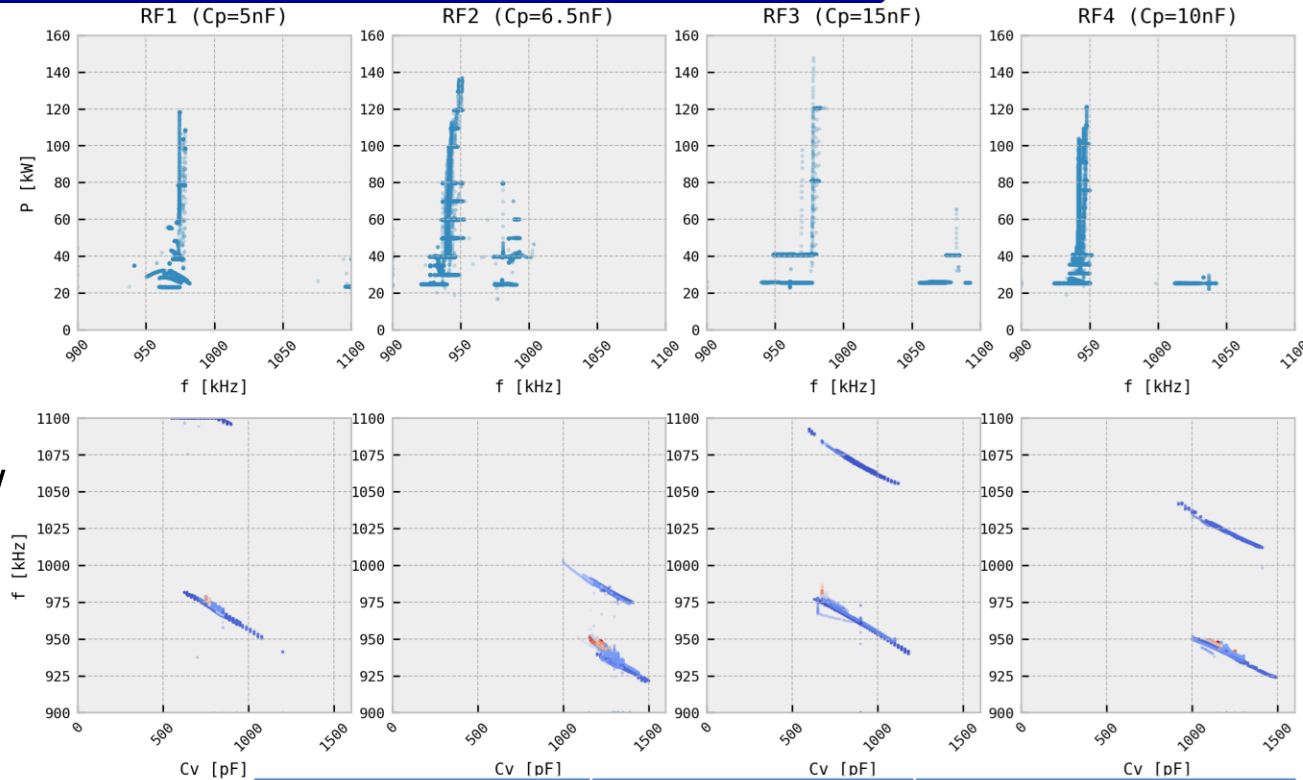


$C_p$ [nF]	$C_v$ [nF] limit
5 (RF #1)	$0.76 \pm 0.05$
6.5 (RF #3)	$0.88 \pm 0.05$
10 (RF #4)	$1.22 \pm 0.05$
15 (RF #2)	$1.3 \pm 0.05$



# Operation of single RF generators

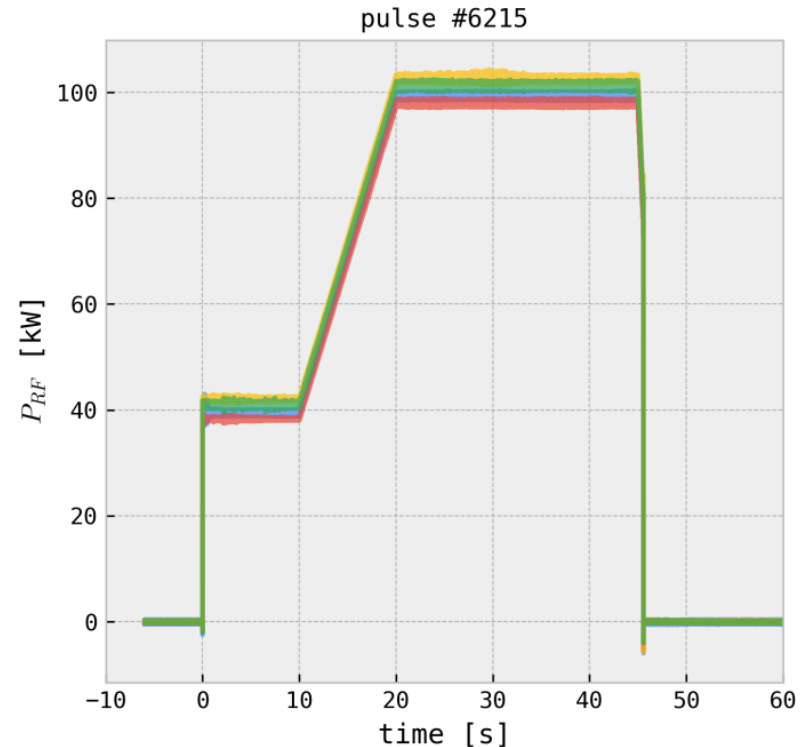
- Hysteresis depending on  $C_v$  observed and modelled
  - best  $C_v$  value near lower flip frequency
- RF power limit depending on  $C_p$  value



$C_p$ [nF]	$C_v$ [nF] limit	Maximum reached $P_{RF}$ [kW]
5 (RF #1)	$0.76 \pm 0.05$	120
6.5 (RF #3)	$0.88 \pm 0.05$	150
10 (RF #4)	$1.22 \pm 0.05$	125
15 (RF #2)	$1.3 \pm 0.05$	135

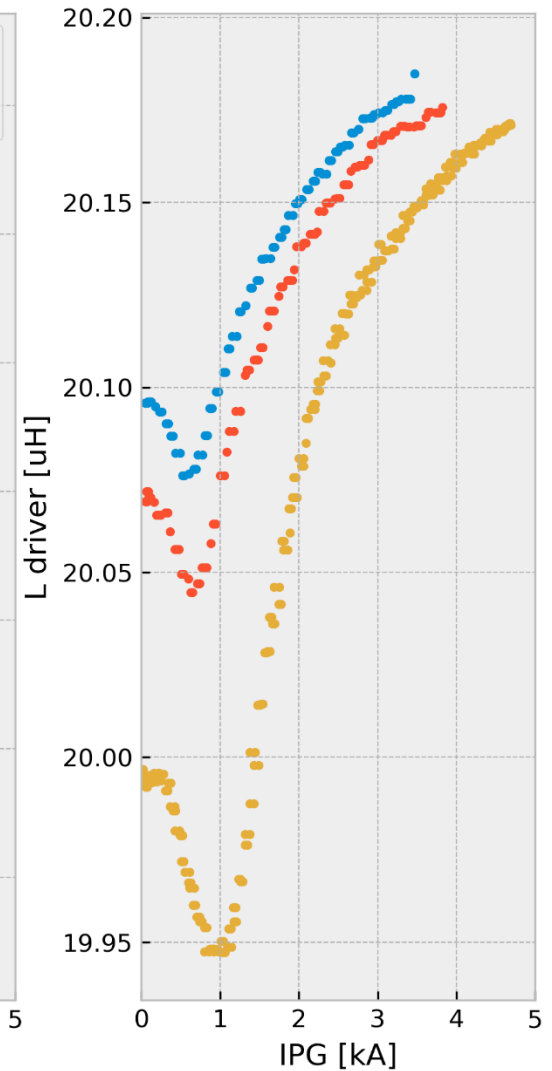
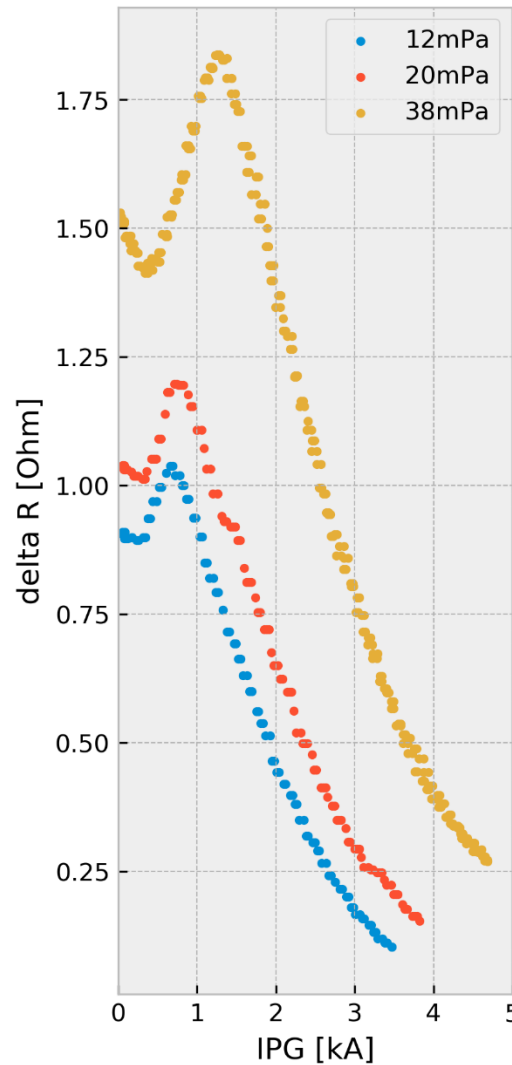
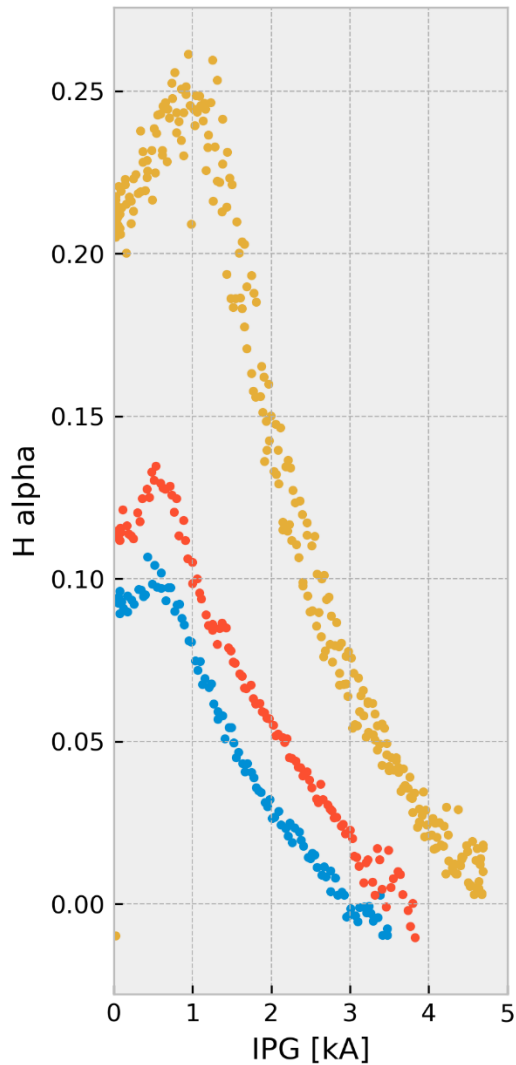


- Hysteresis depending on  $C_v$  observed and modelled
  - best  $C_v$  value near lower flip frequency
- RF power limit depending on  $C_p$  value
- Simultaneous operation of 4 RF generators:
  - max RF power 100kW so far

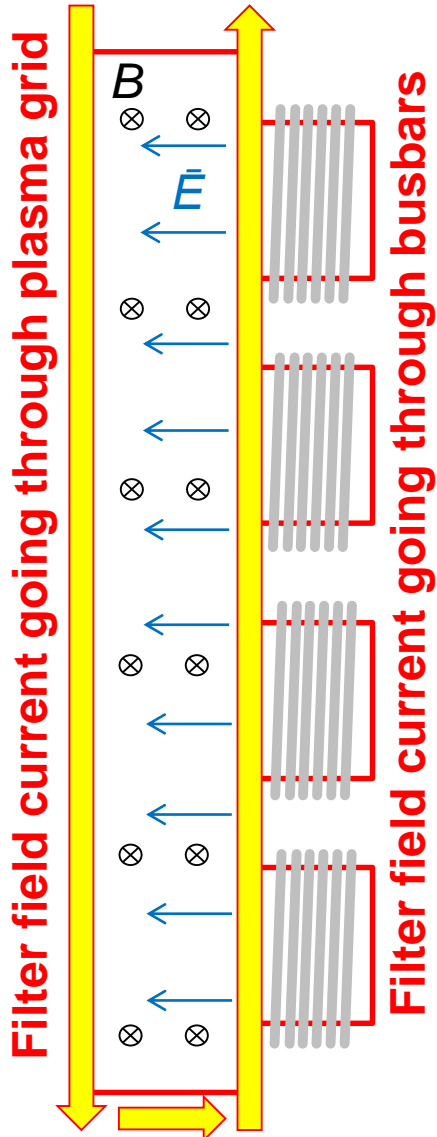


$C_p$ [nF]	$C_v$ [nF] limit	Maximum reached $P_{RF}$ [kW]
5 (RF #1)	$0.76 \pm 0.05$	120
6.5 (RF #3)	$0.88 \pm 0.05$	150
10 (RF #4)	$1.22 \pm 0.05$	125
15 (RF #2)	$1.3 \pm 0.05$	135

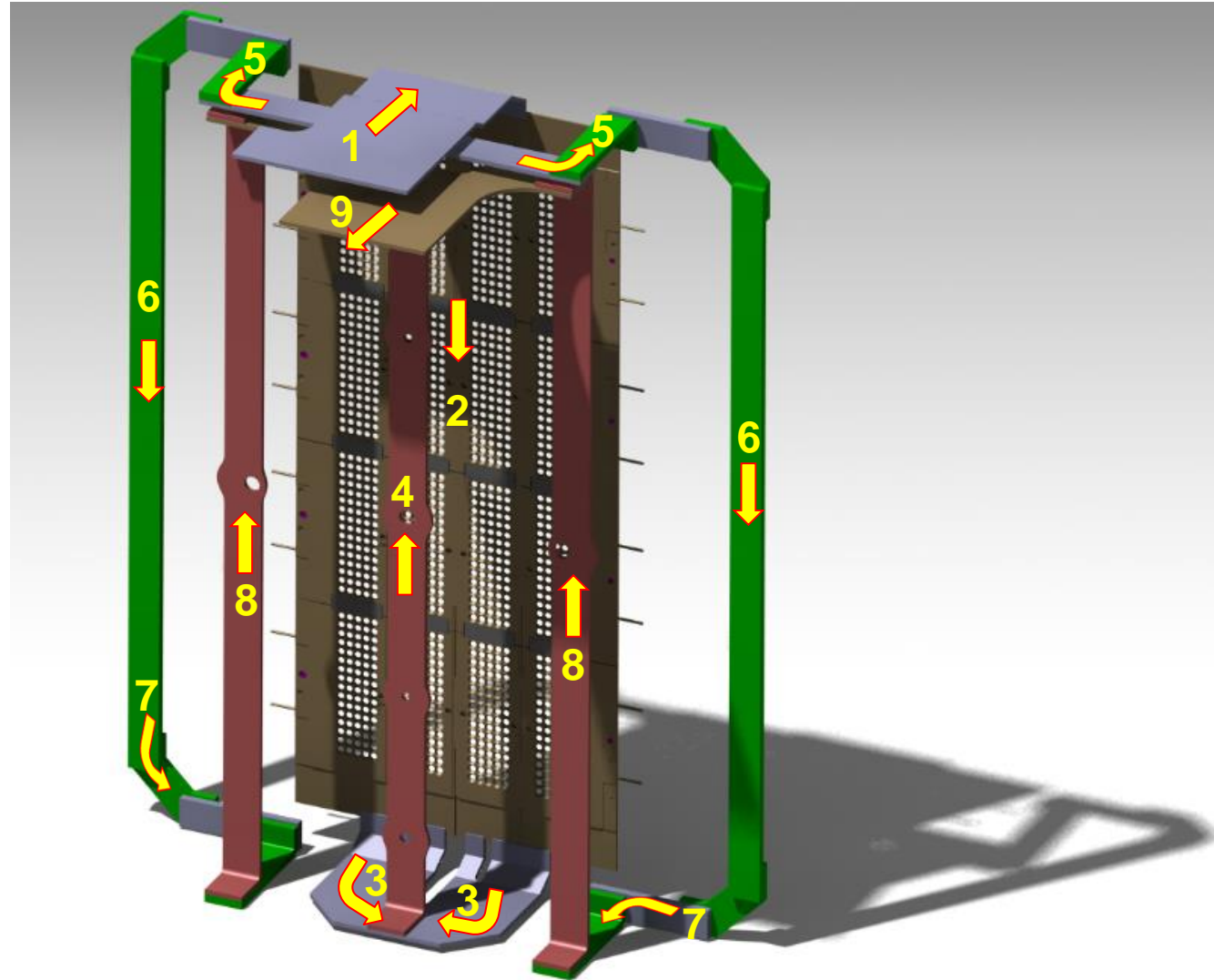
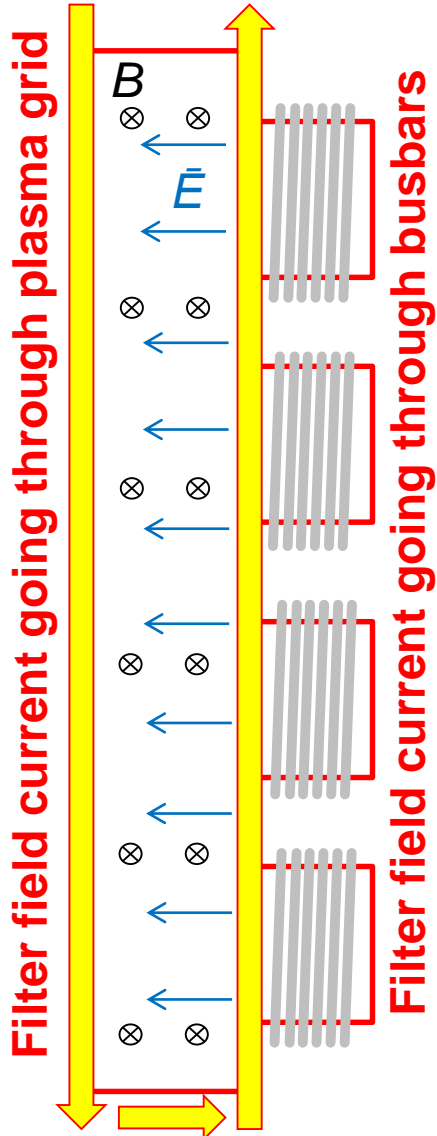
## ● Effect of filter field on driver plasma



- Schematic path of filter field current

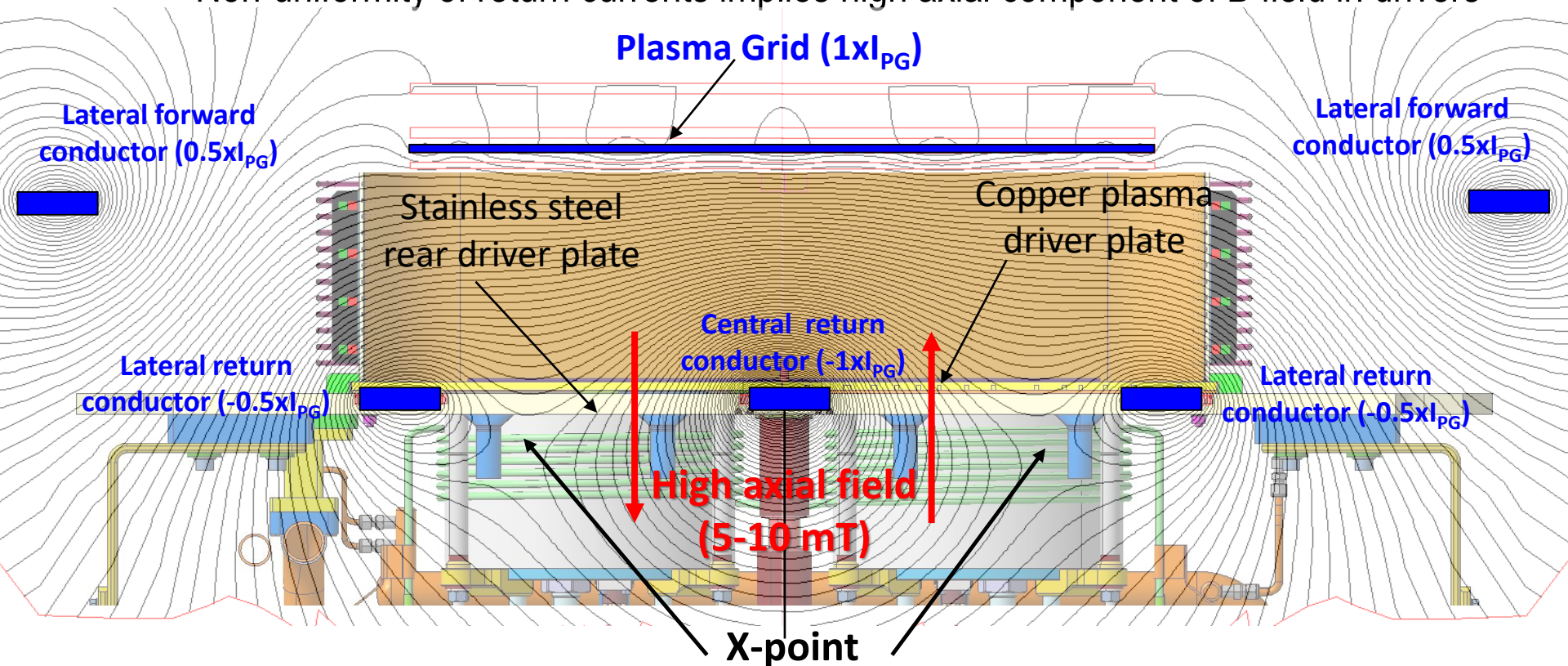


- Detailed path of filter field current



- Present filter field configuration:

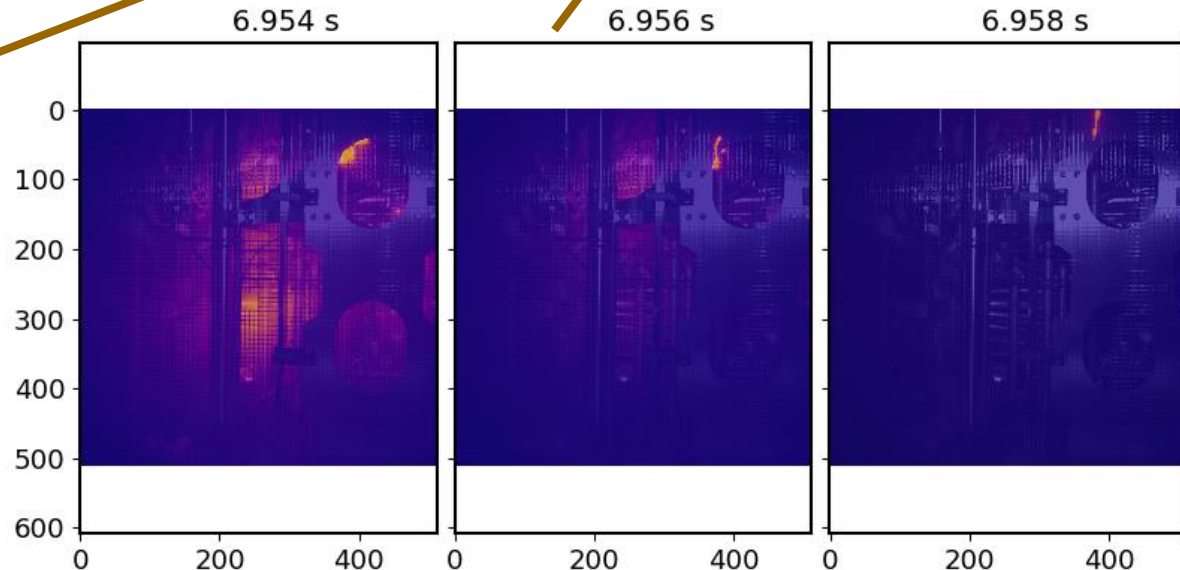
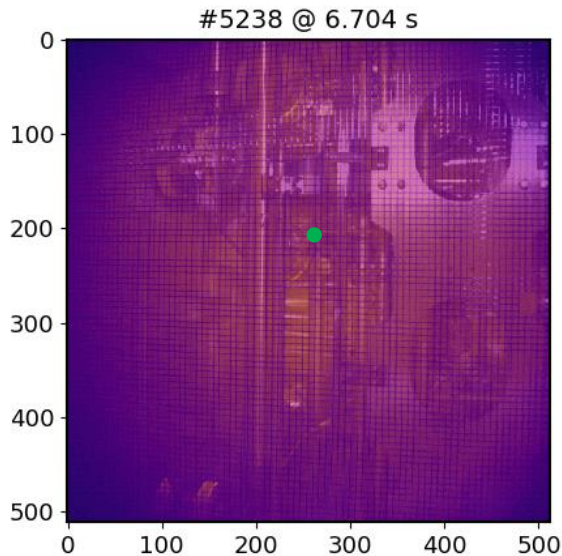
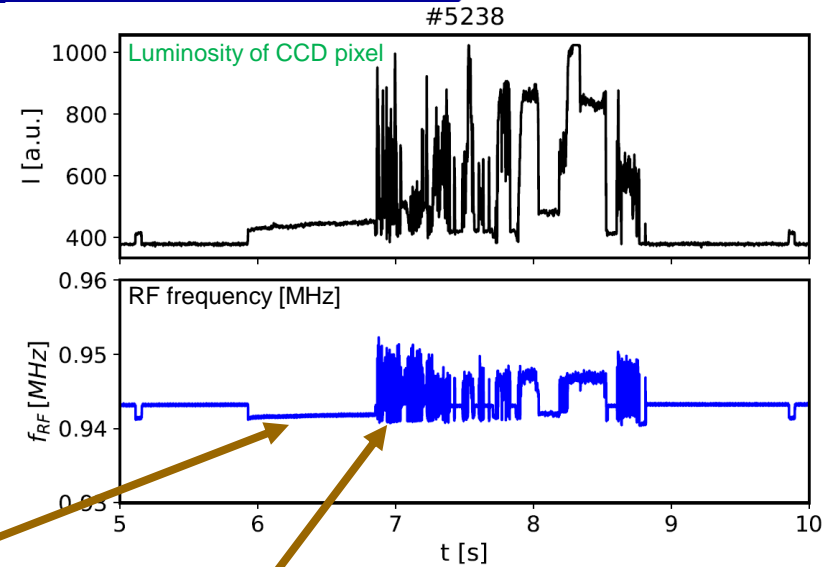
- PG busbar layout designed for: max B field strength and **uniformity** in plasma source (upstream of PG), B field **parallel** to PG, low B field in drivers
- Non-uniformity of return currents implies high axial component of B field in drivers





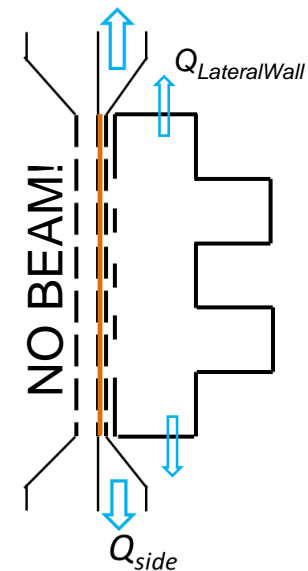
# RF breakdown outside plasma chamber

- Beam source in vacuum
- Breakdown on source rear side due to RF:
  - analysis by fast cameras
  - investigation of pressure effect





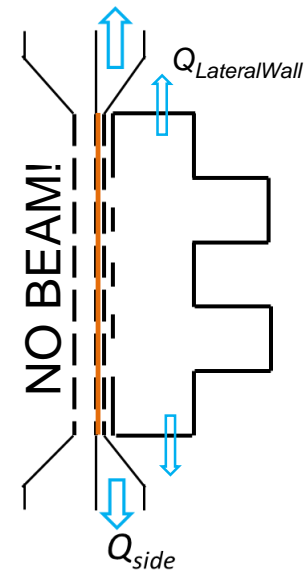
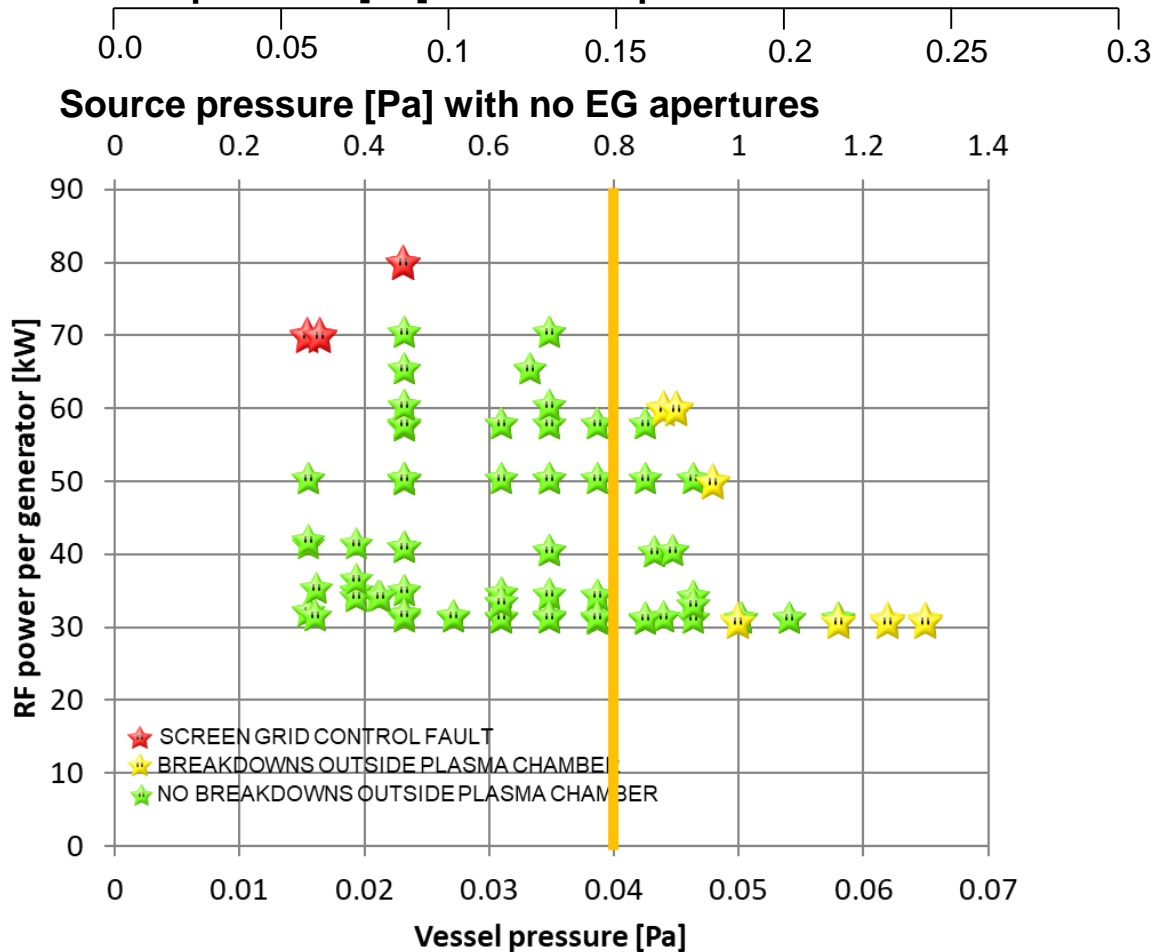
- Hypothesis: RF breakdowns induced by large background gas pressure
- Installation of mask on upstream side of EG
  - all EG apertures blinded



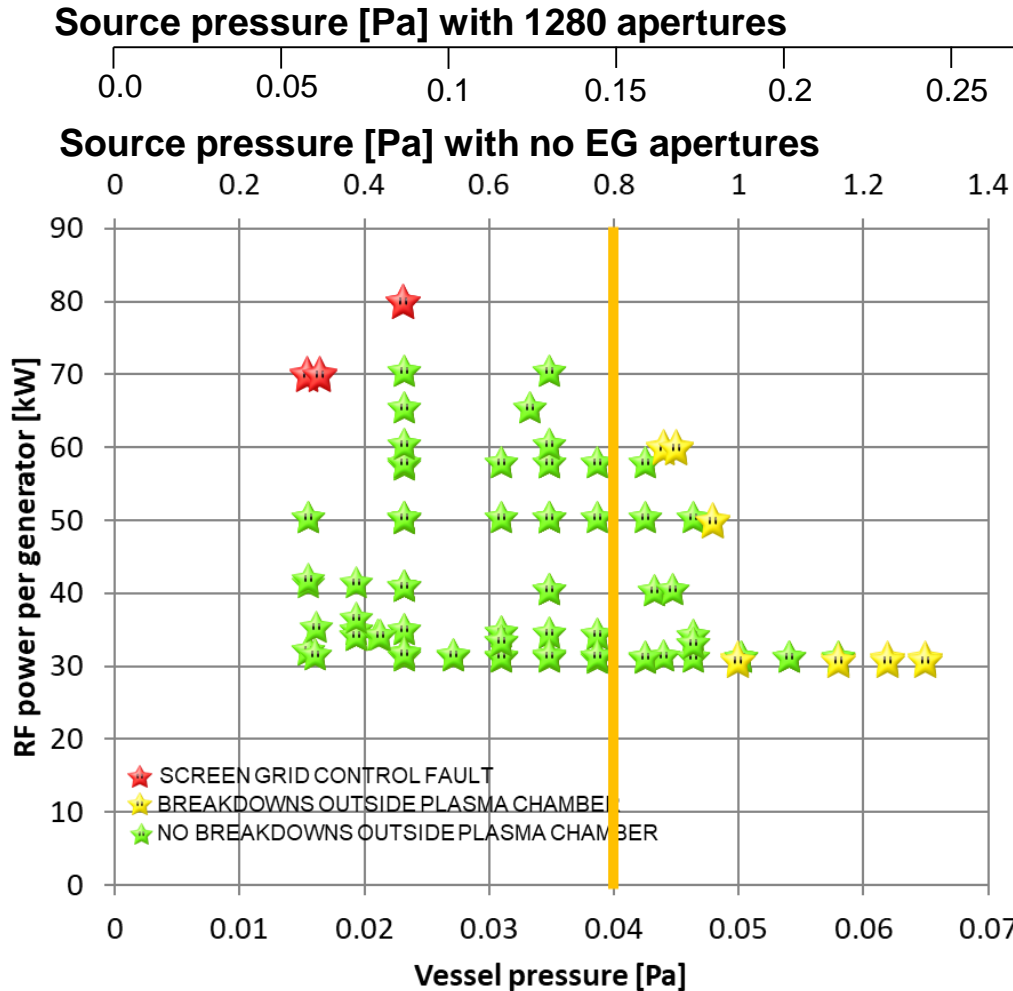
- Identification of discharge conditions vs background gas pressure

Source pressure [Pa] with 1280 apertures

Source pressure [Pa] with no EG apertures



- Identification of discharge conditions vs background gas pressure



$p_{vessel} \approx 40 \text{ mPa}$   
 seems threshold for  
 RF discharges

- More powerful pumping system required
- Long time scale

M. Siragusa et al., Numerical simulation of experimental tests performed on ZAO® Non-EvaporableGetter pump designed for NBI applications, ICIS2019, poster WedP50

M. Siragusa et al., Simulation of the gas density distribution in the accelerator of the ELISE test facility, ICIS2019, poster WedP15

# RF breakdown outside plasma chamber

Source pressure [Pa] with 80 PG apertures

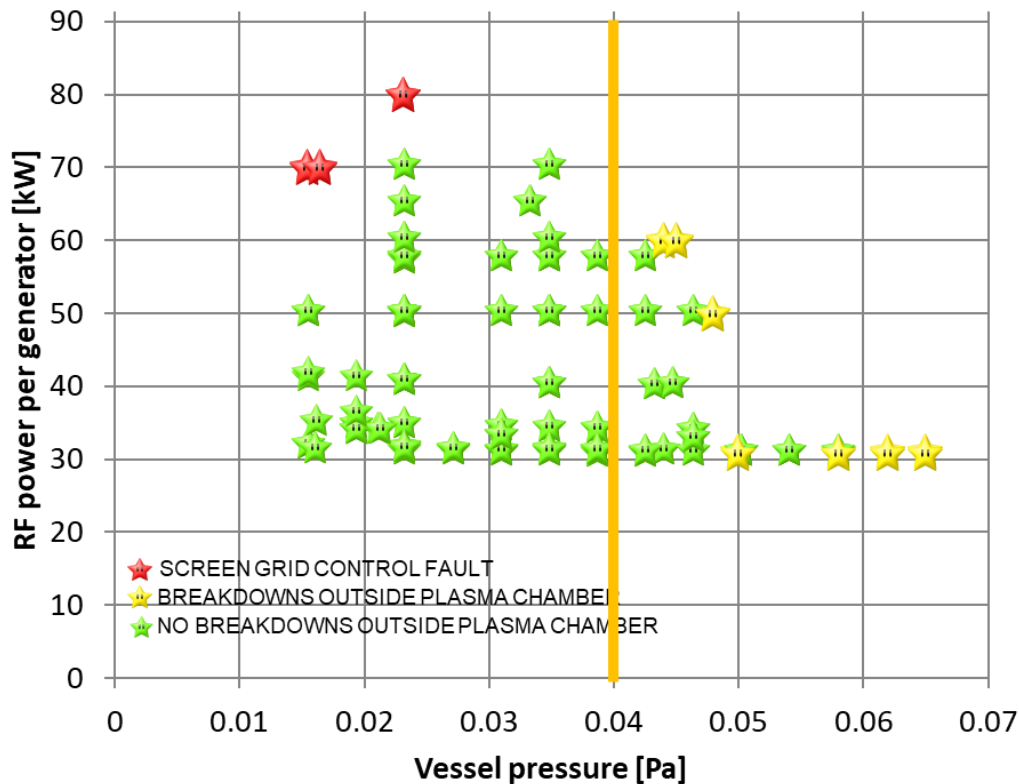
0.0 0.1 0.2 0.3 0.4 0.5

Source pressure [Pa] with 1280 apertures

0.0 0.05 0.1 0.15 0.2 0.25 0.3

Source pressure [Pa] with no EG apertures

0 0.2 0.4 0.6 0.8 1 1.2 1.4



- In the meantime:
  - installation of plasma grid mask
  - number of beamlet determined by numerical simulations

# Installation of plasma grid mask

- No access from plasma side
- Installation between PG and EG

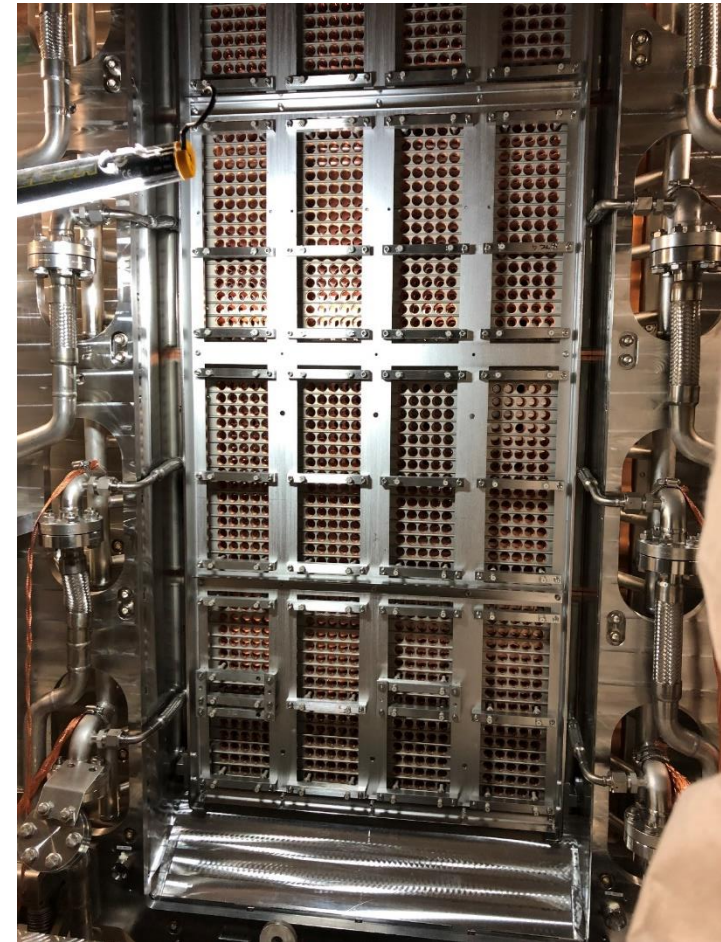
Molybdenum plate 0.25mm thick



Pushers press mask against PG, acting from GG  
Pyrex pushers to be installed in view of Cs operation



View from downstream



A. Maistrello et al., Voltage Hold Off Test of the Insulating Supports for the Plasma Grid Mask of SPIDER, ISFNT2019, subm. Fusion Eng. Des.

M. Pavei et al., SPIDER Plasma Grid masking for reducing gas conductance and pressure in the Vacuum Vessel, ISFNT2019, subm. Fusion Eng. Des.



## Source diagnostics:

### Electrical currents

### Calorimetry and surface thermocouples **M** **HNB**

(dissipated power & local load on components)

### Electrostatic probes

(plasma uniformity,  $T_e$ ,  $n_e$ )

### Source optical emission spectroscopy **M**

(source plasma  $T_e$ ,  $n_e$ ,  $n_{H^-}$ ,  $n_{Cs}$ ,  $n_H$ , impurities),

CRDS ( $n_{H^-}$ ), Laser absorption ( $n_{Cs}$ ) **M**

## Beam diagnostics:

### Calorimetry and surface thermocouples **M** **HNB**

(beam uniformity, diverg., aiming, vert. resol. 70 mm)

### Instrumented calorimeter **STRIKE**

(beam uniformity over 2D profile & divergence, resolution 2mm, < 10 s beam pulse, SPIDER only )

### Beam emission spectroscopy **M**

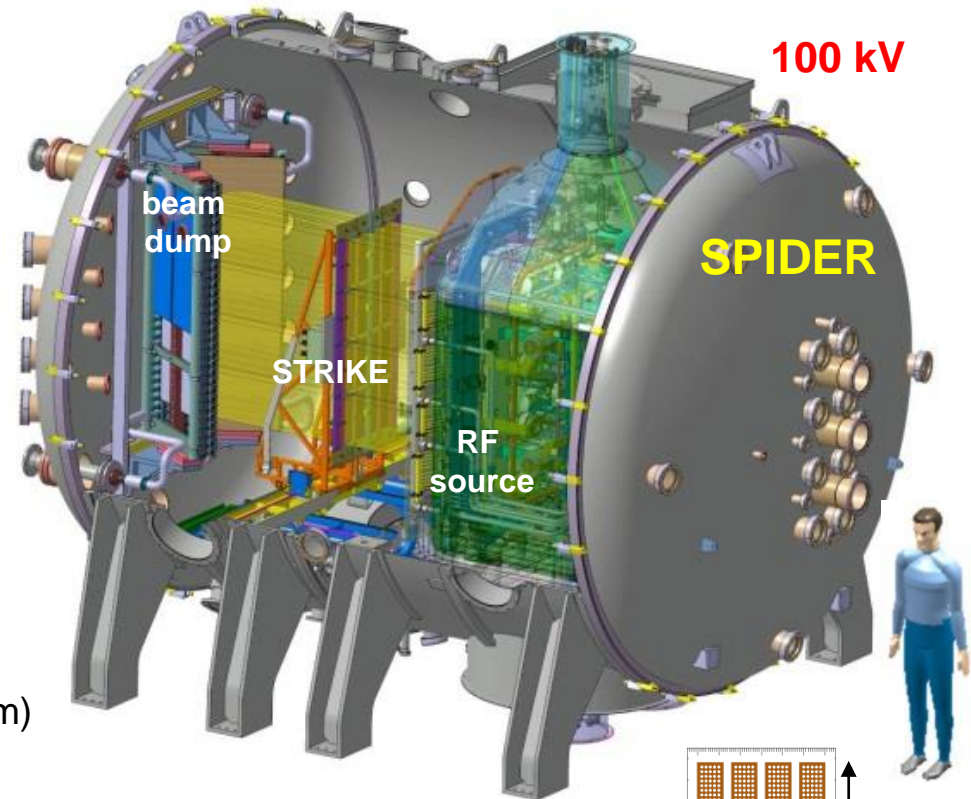
(beam divergence, stripping losses, uniformity)

### Beam tomography **M**

(beam uniformity over 2D profile, resolution 1/4 beamlet group)

### Neutron imaging **M**

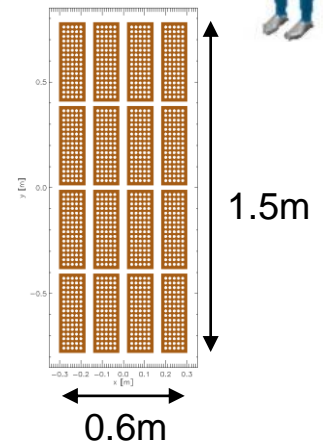
(beam uniformity profile, resolution 3-4 cm, D only)



Also available in:

**M – MITICA**

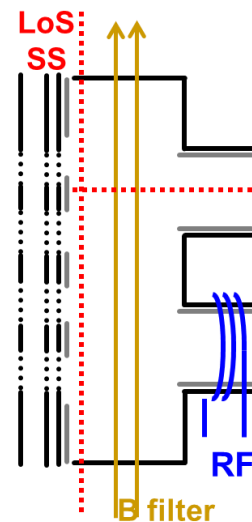
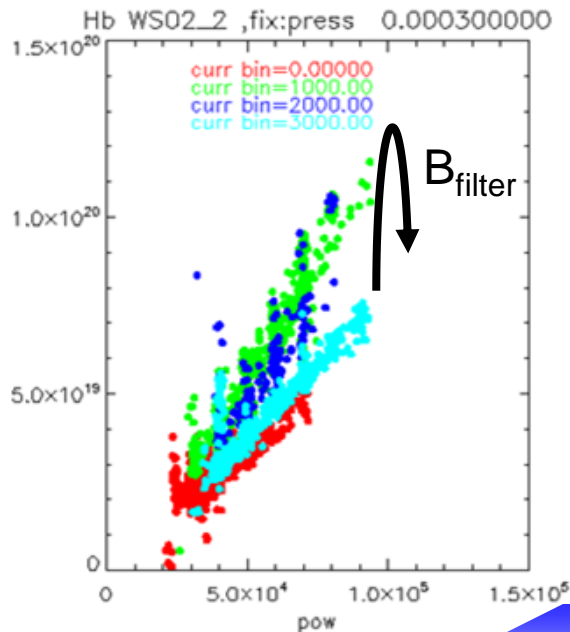
**HNB – ITER injector**



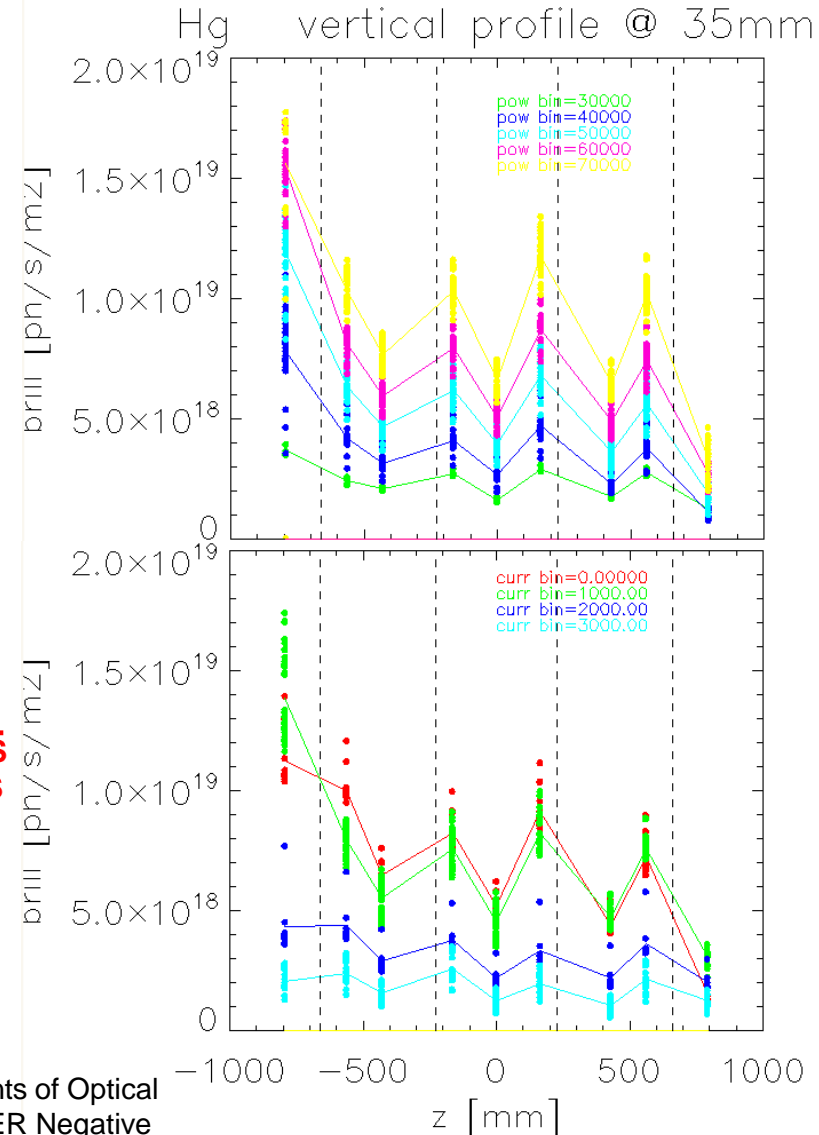
R. Pasqualotto et al.,  
JINST 12 (2017) C10009



- Both in driver and close to PG, emission increases with RF power and decreases with magnetic filter field
  - Emission dependence on magnetic filter inside drivers due to return currents
- Plasma emission increases towards bottom

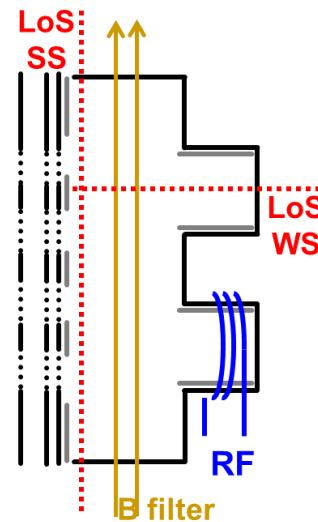
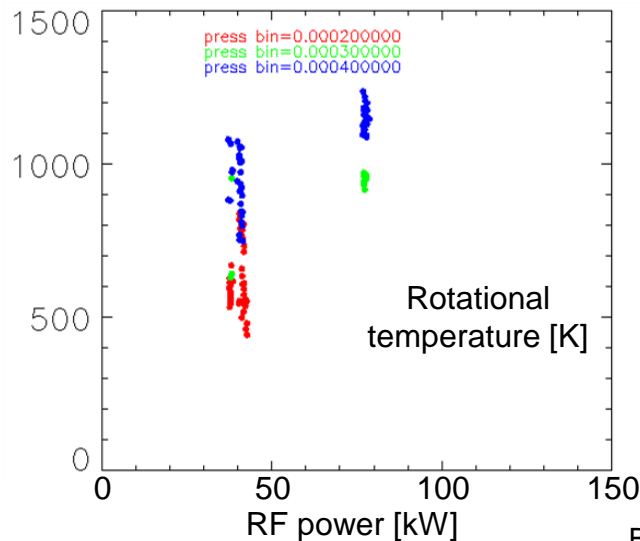
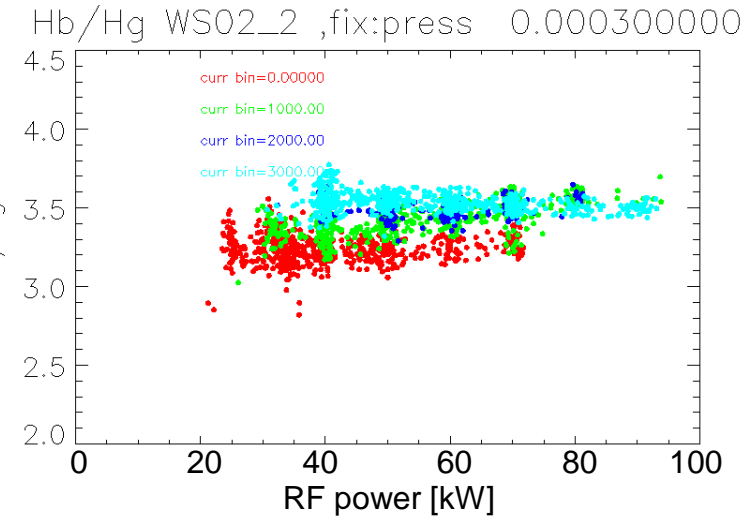


B. Zaniol et al., First measurements of Optical Emission Spectroscopy on SPIDER Negative Ion Source, ICIS2019, poster WedP13

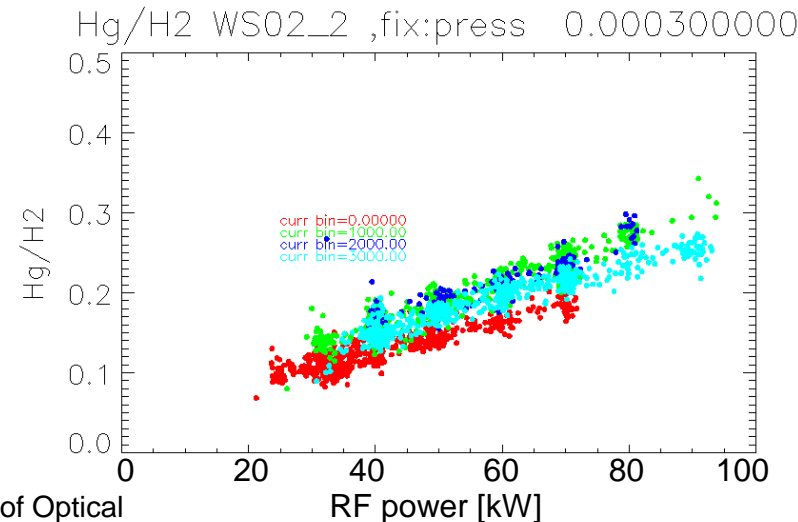


# Preliminary characterisation of ion source

- No clear dependence of  $H_{\text{beta}}/H_{\text{gamma}}$  on RF power
- Increase of  $H_{\text{gamma}}/\text{Fulcher}$  with RF power
- $T_{\text{rot}}$  increasing with RF power and pressure
- No effect of extraction on spectroscopy



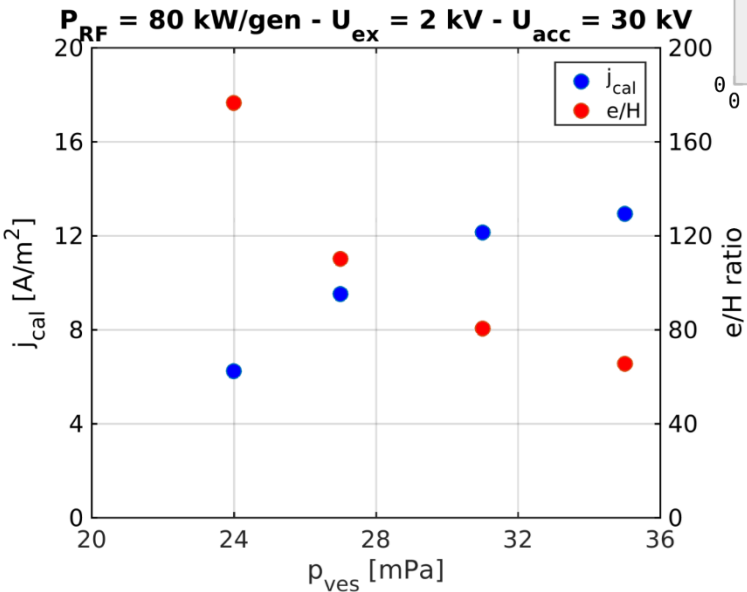
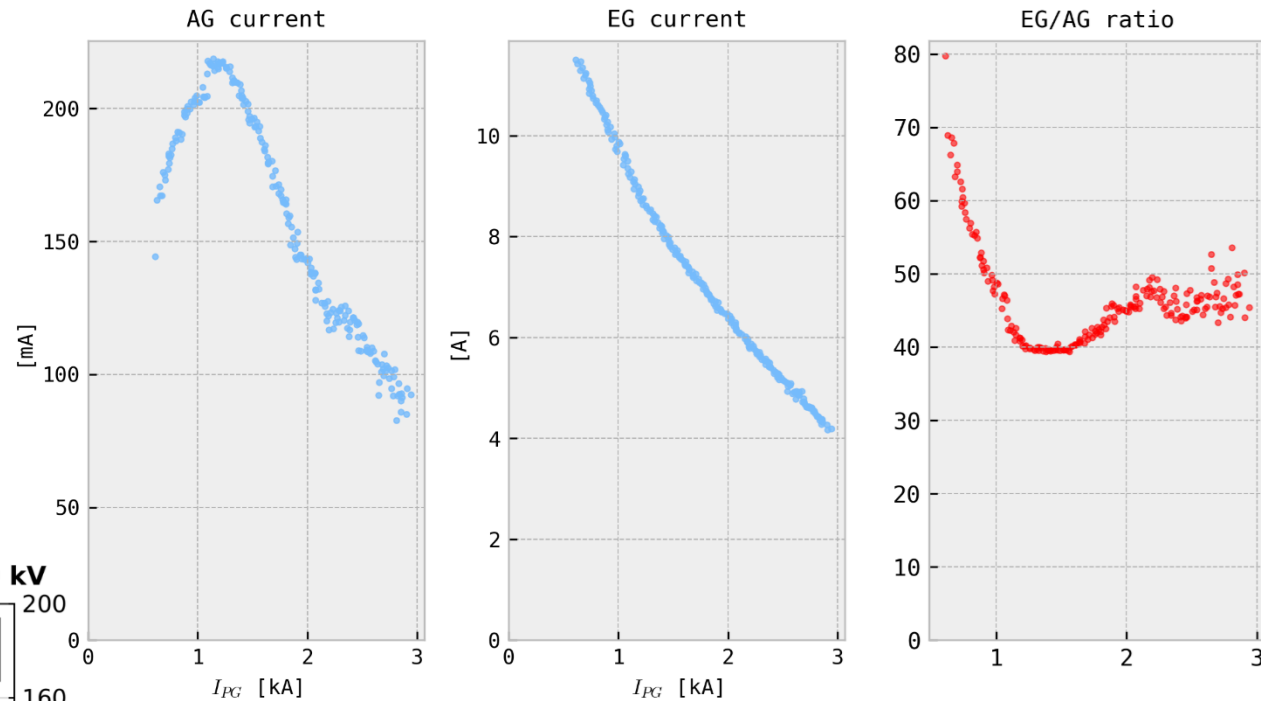
B. Zaniol et al., First measurements of Optical Emission Spectroscopy on SPIDER Negative Ion Source, ICIS2019, poster WedP13



# Characterisation of co-extracted electrons

pulse 6038  $U_{EG} = 1.5\text{kV}$   $U_{AG} = 20\text{kV}$

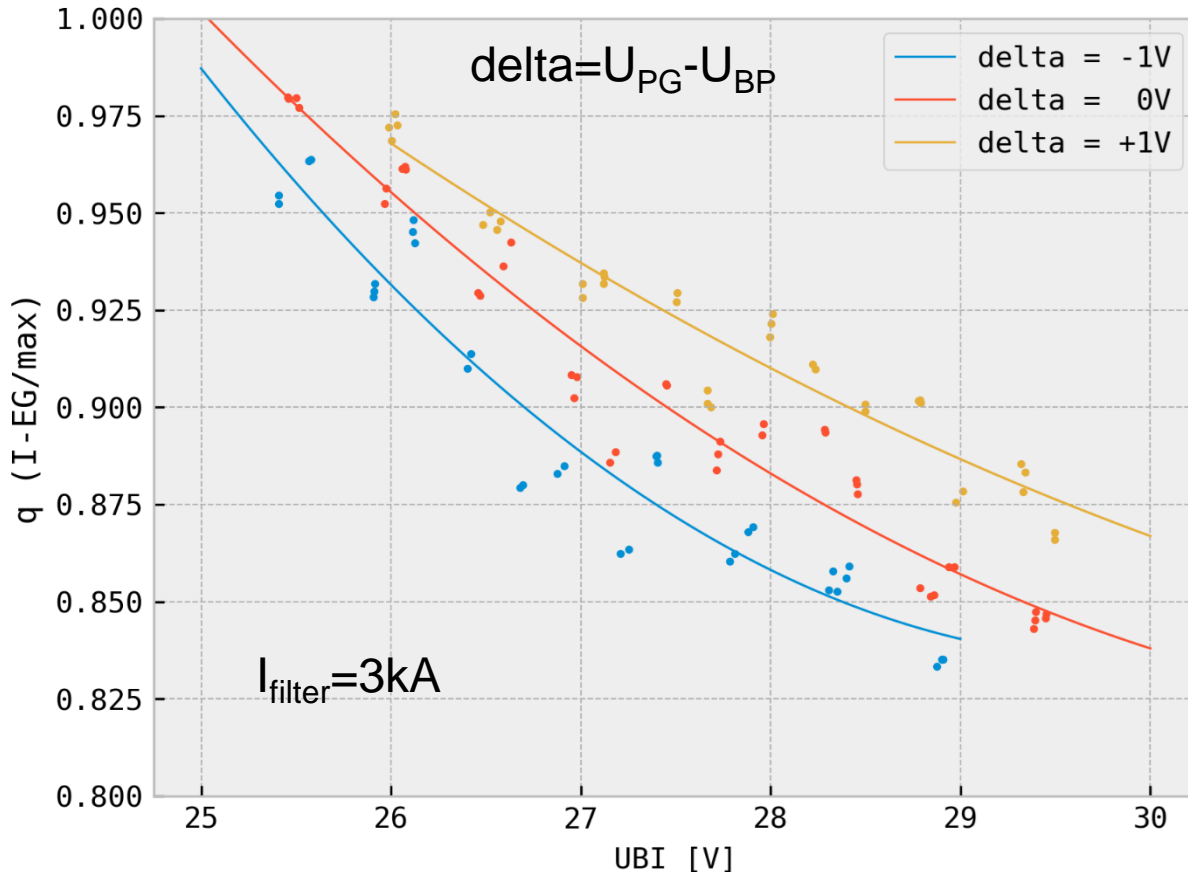
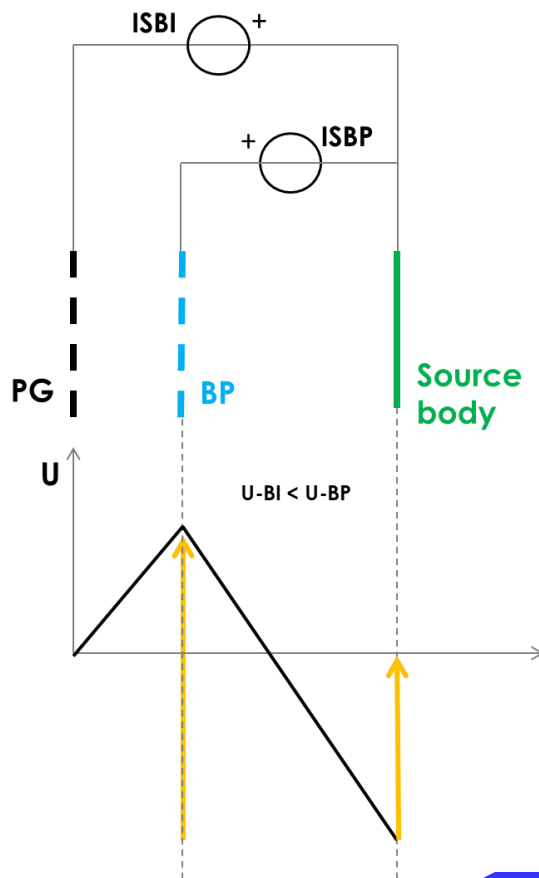
- Optimal B field for minimum current ratio



- Decay of co-extracted electron current wrt pressure

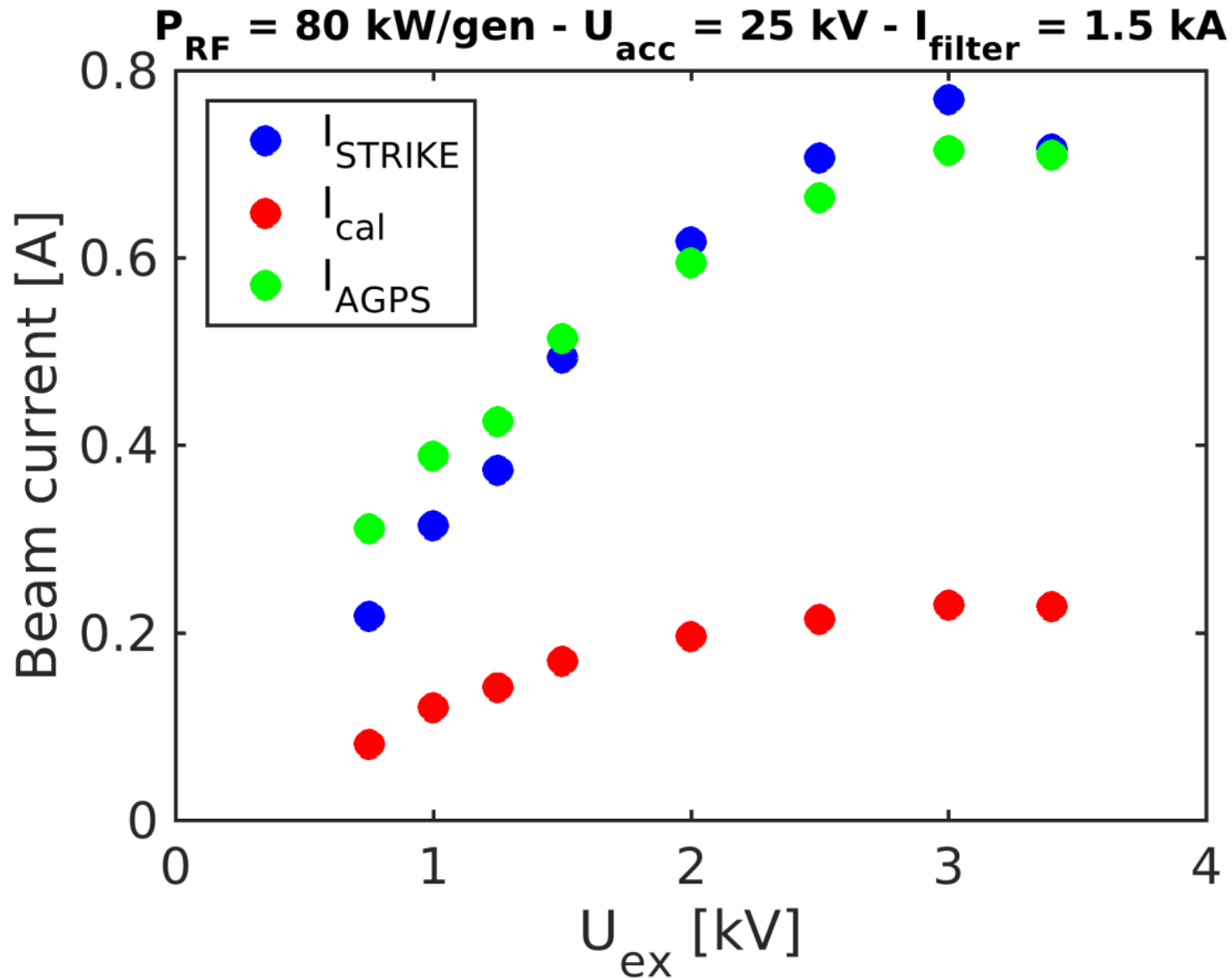
- Bias of plasma grid and bias plate:

- With no caesium plasma potential can exceed limit of power supplies (30V)
- Verification of influence on co-extracted electrons (low RF power, large filter field)

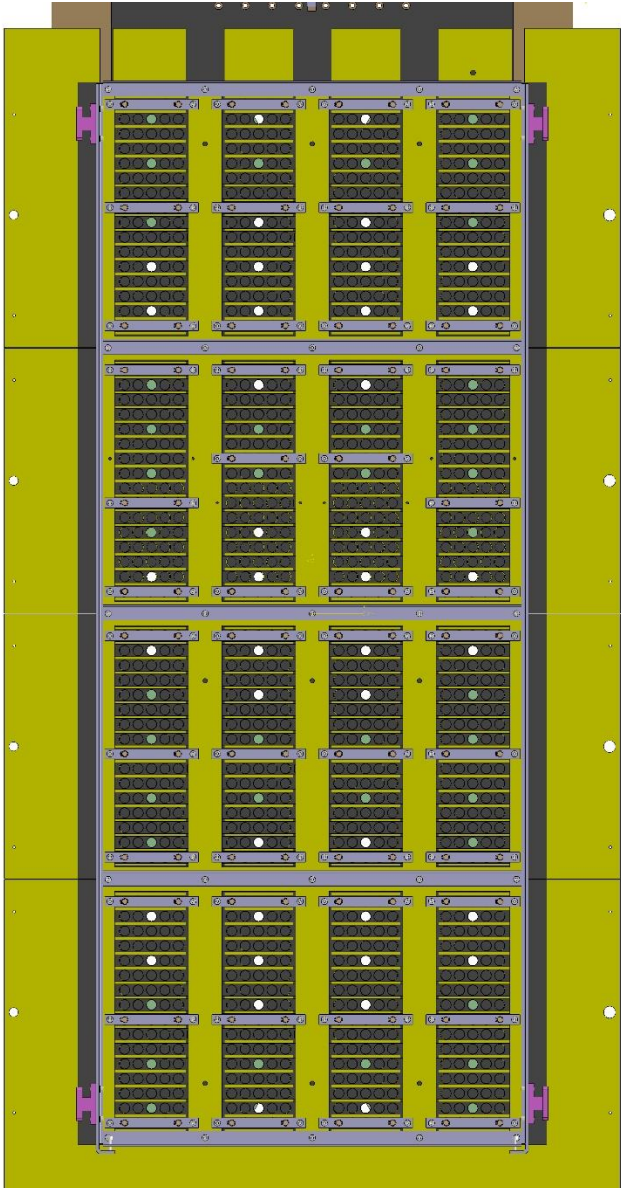




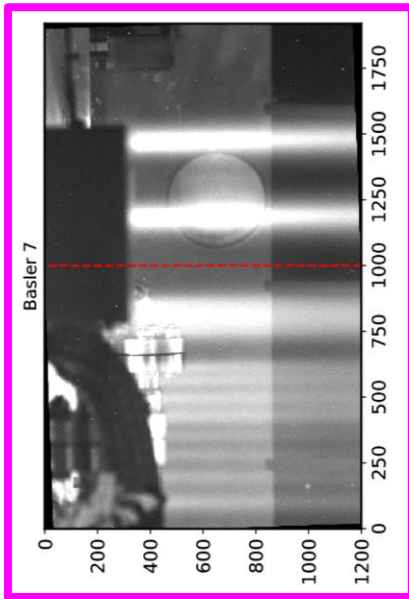
# Characterisation of beam by AGPS current



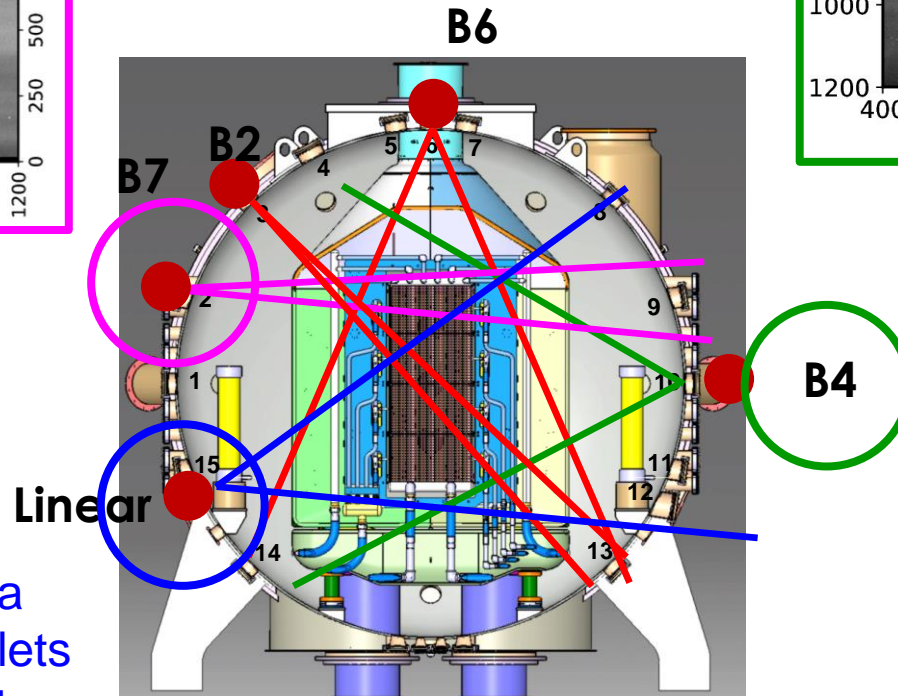
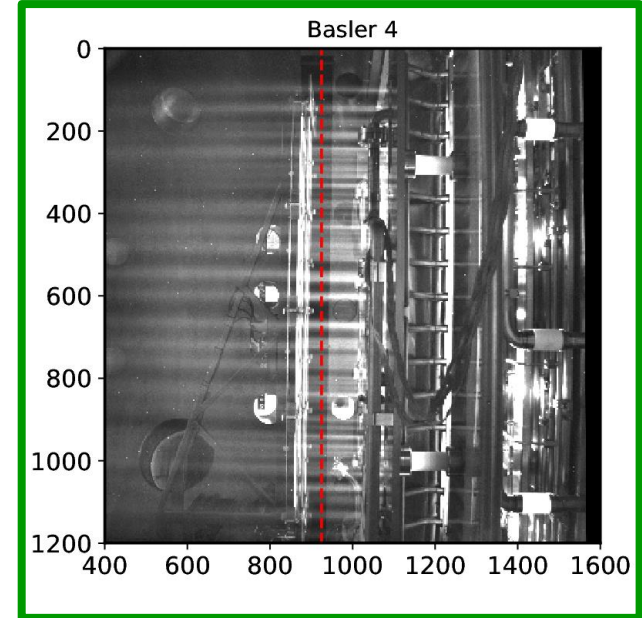
# Operating beamlets



# Characterisation of beam by visible imaging



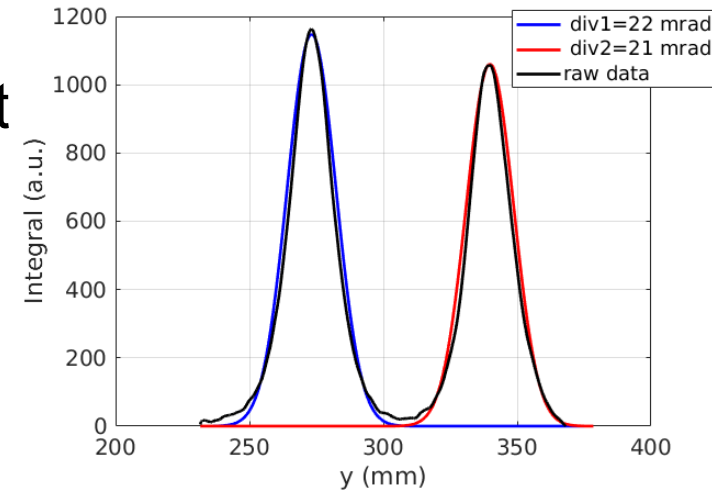
B2 observes first beamlets of segment 1



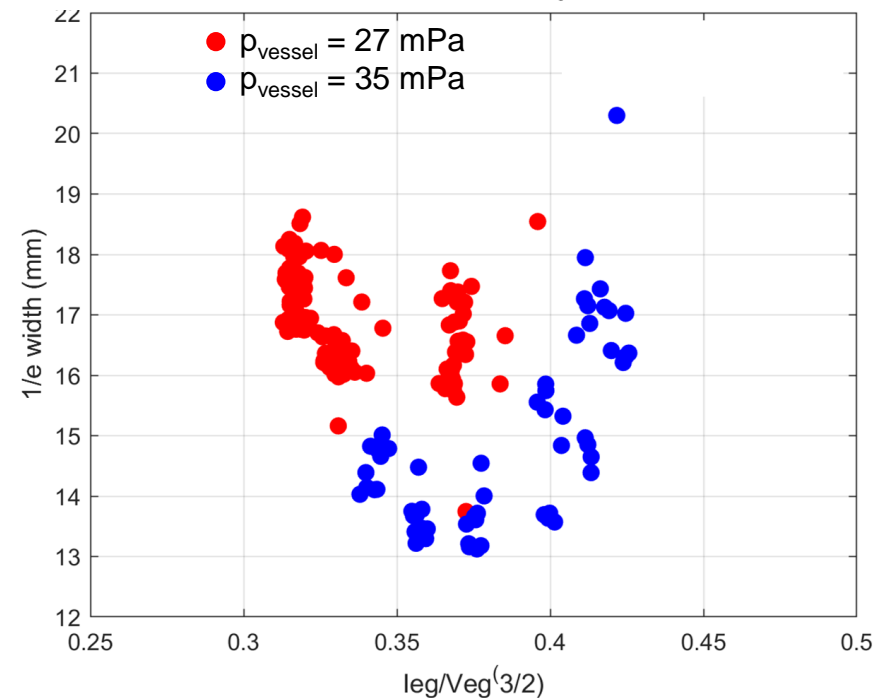
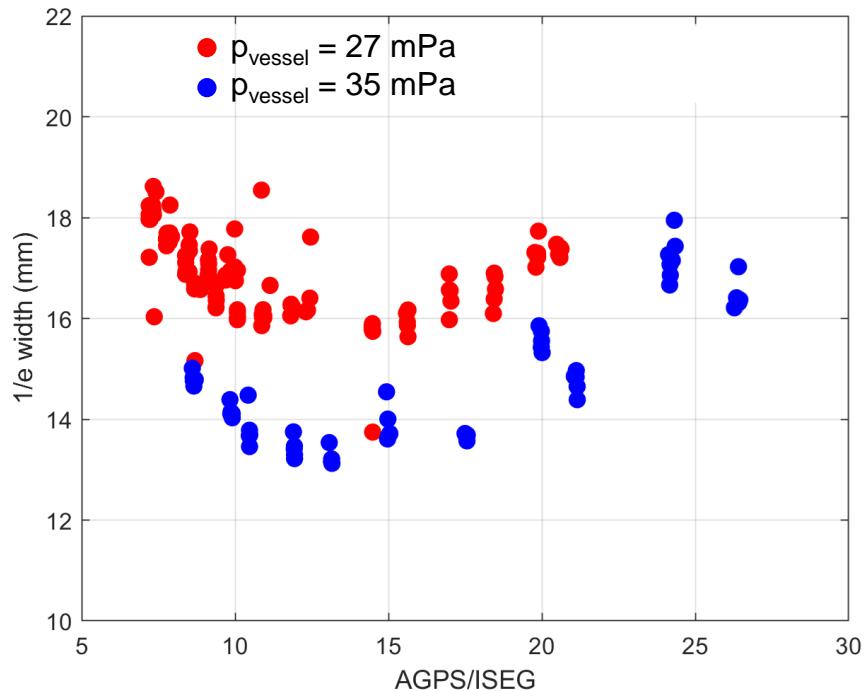
B4 observes: last beamlets of segment 2 and first beamlets of segment 3

Linear camera observes beamlets of segment 4

- Example of experimental data and corresponding fit

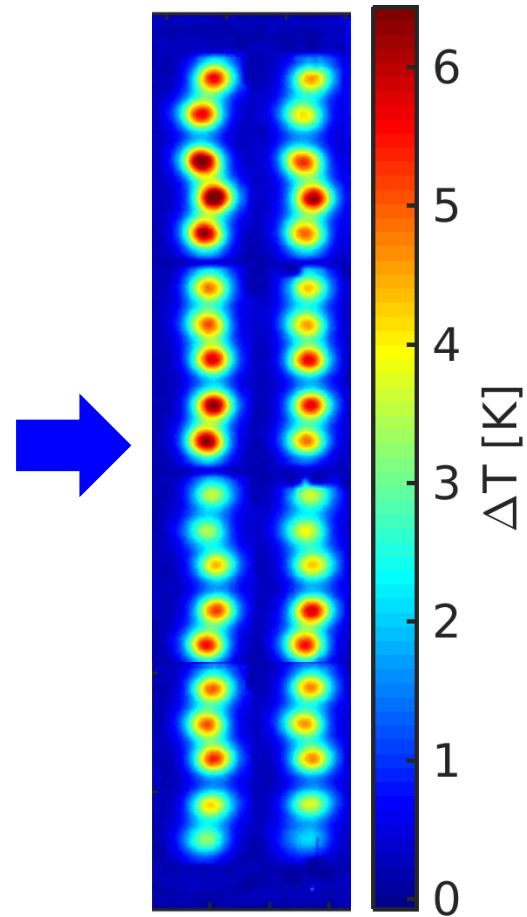
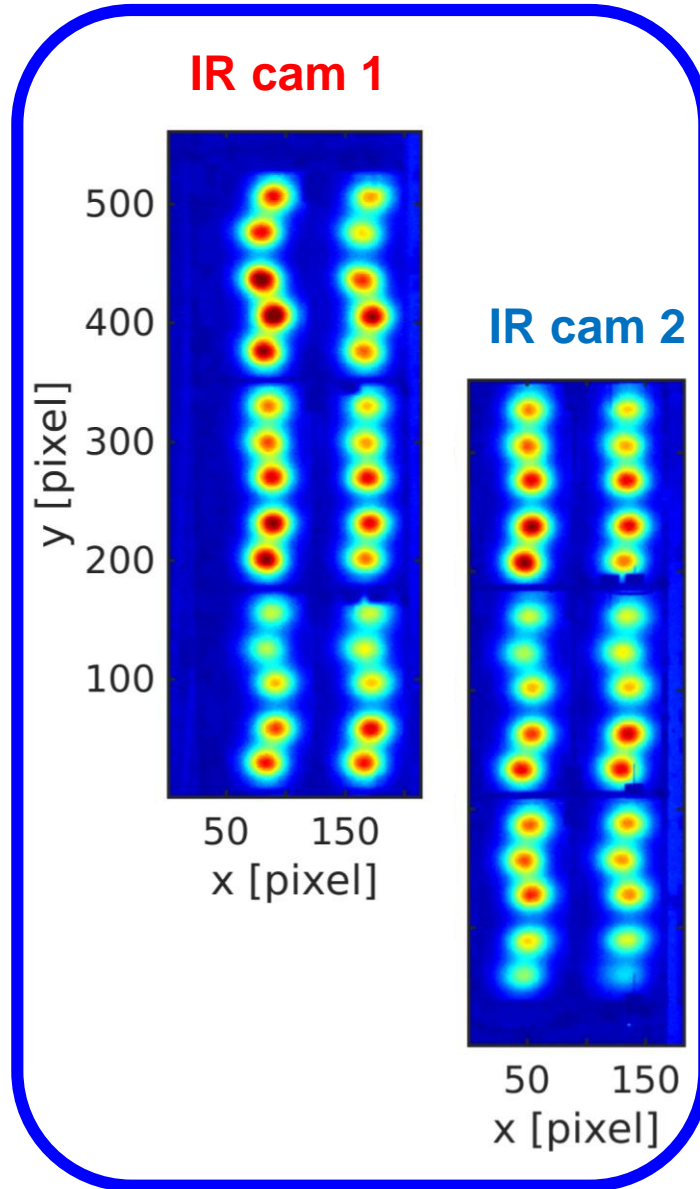
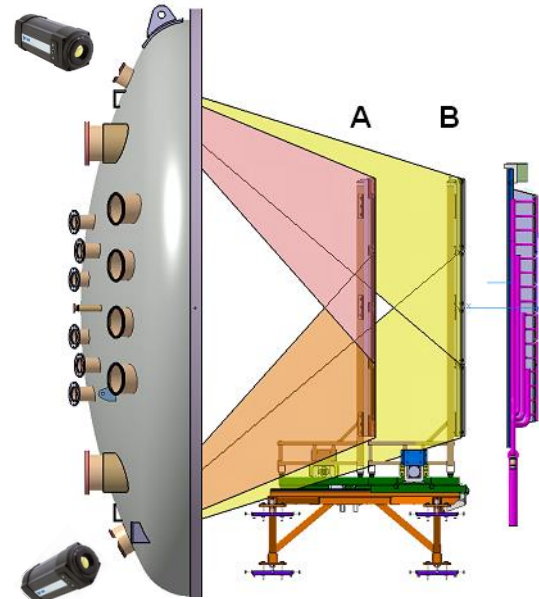
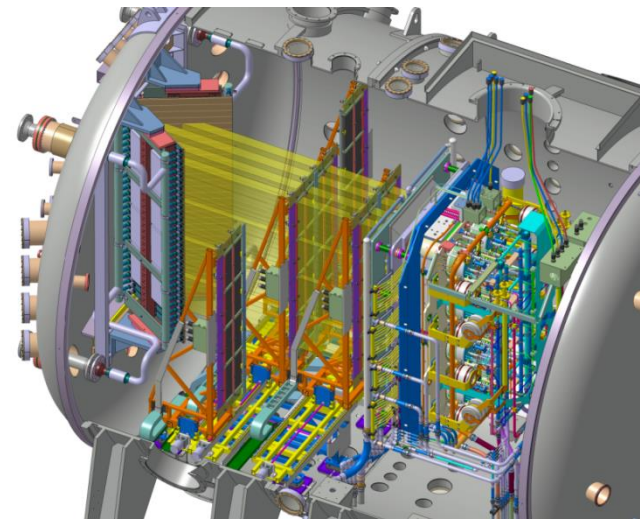


- Divergence vs ratio of acceleration and extraction voltages ; divergence vs normalised perveance





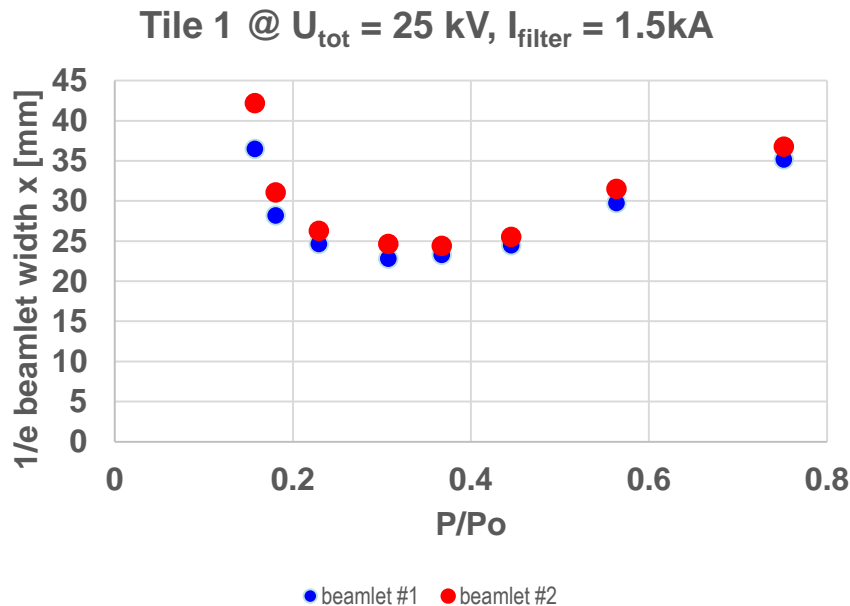
# Characterisation of beam by STRIKE thermography



# Characterisation of beam by STRIKE thermography

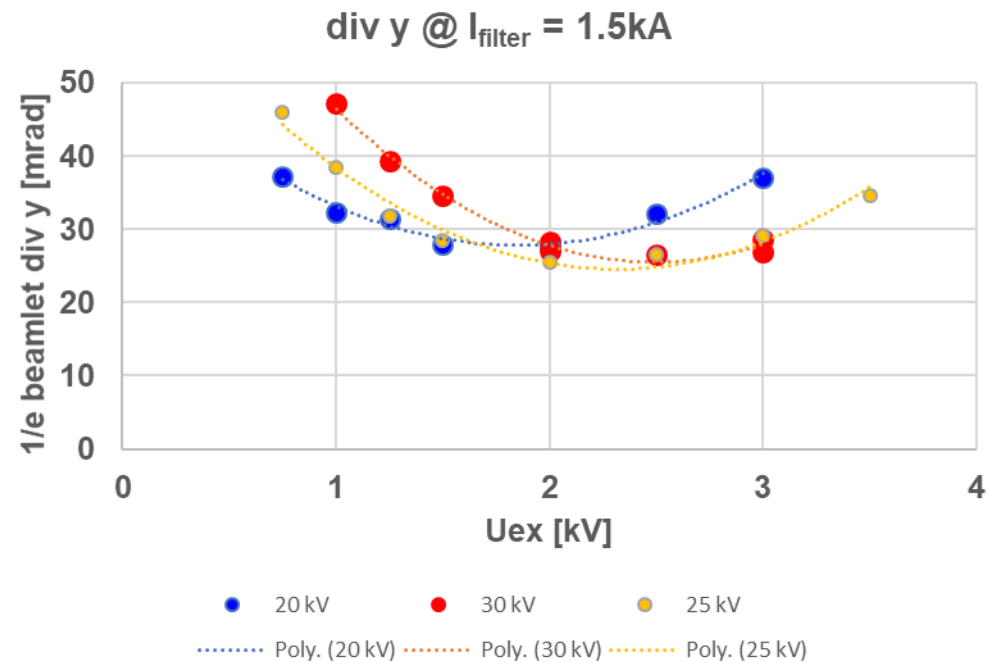
Pulse: #6246-#6250

X width of first two beamlets on Tile 1



Y DIVERGENCE at different  $U_{tot}$

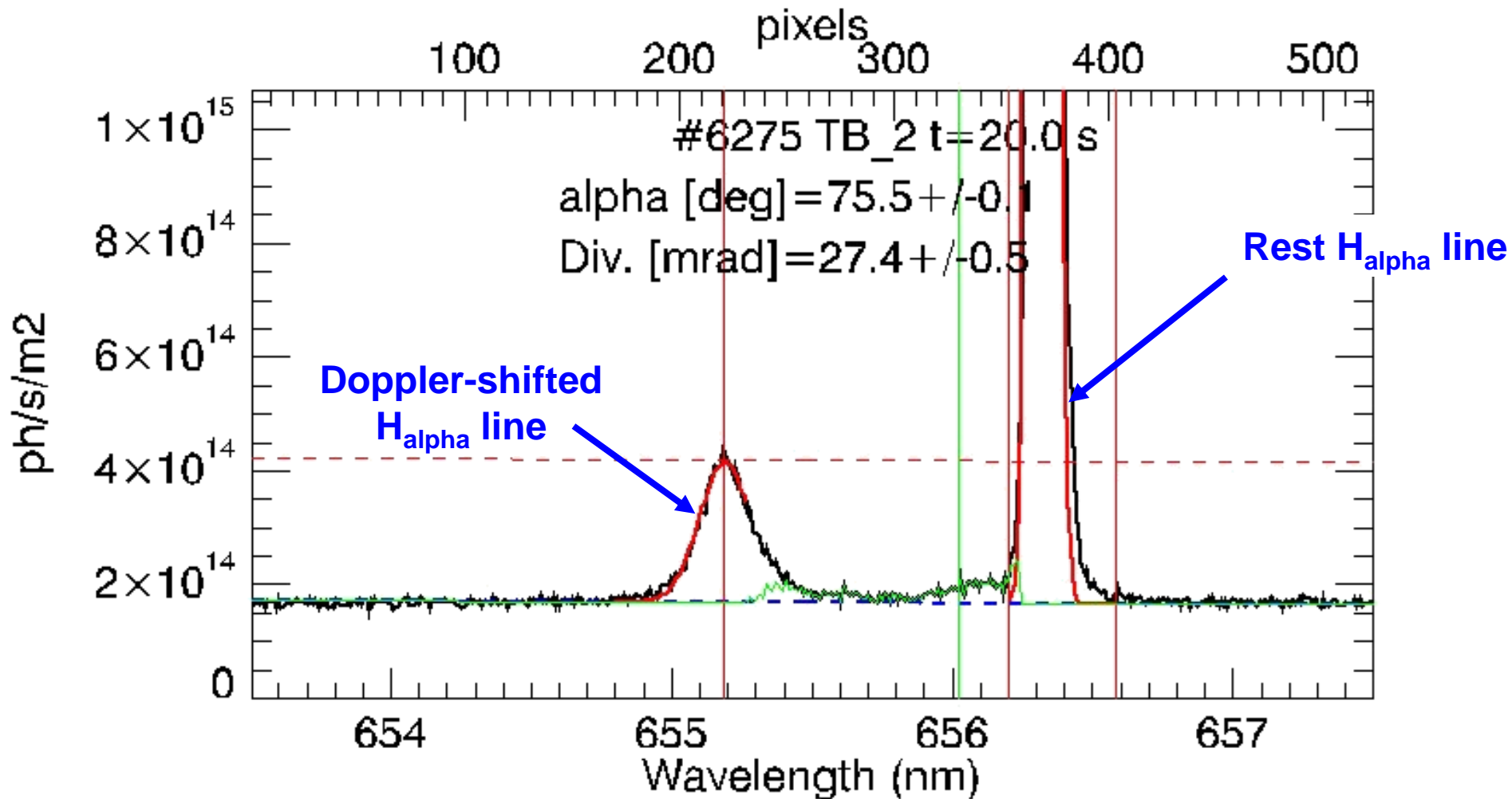
Pulses: #6229-#6243 and #6246-#6250



A Pimazzoni et al., Assessment of the SPIDER beam features by diagnostic calorimetry and thermography, ICIS2019, poster WedP32

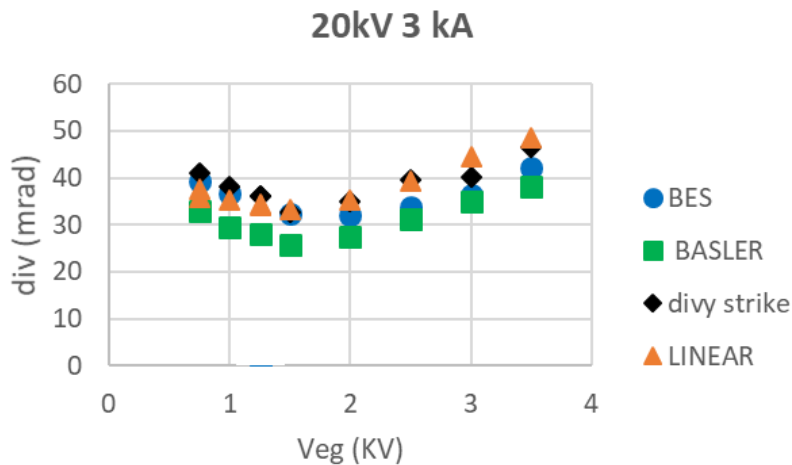
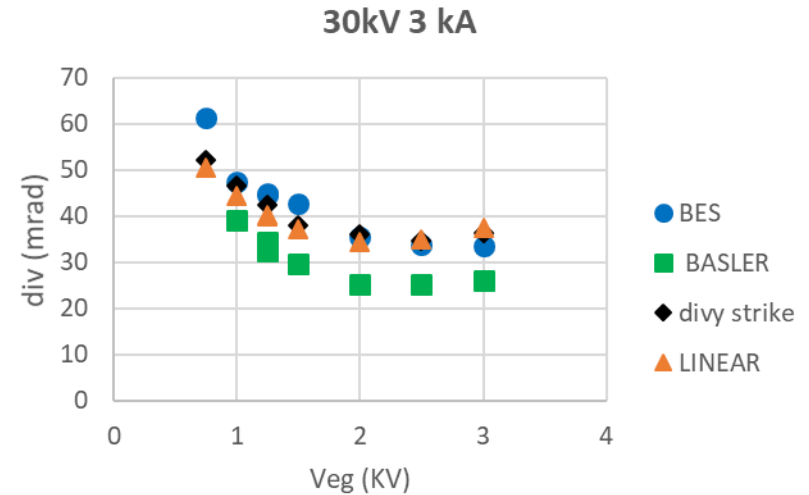
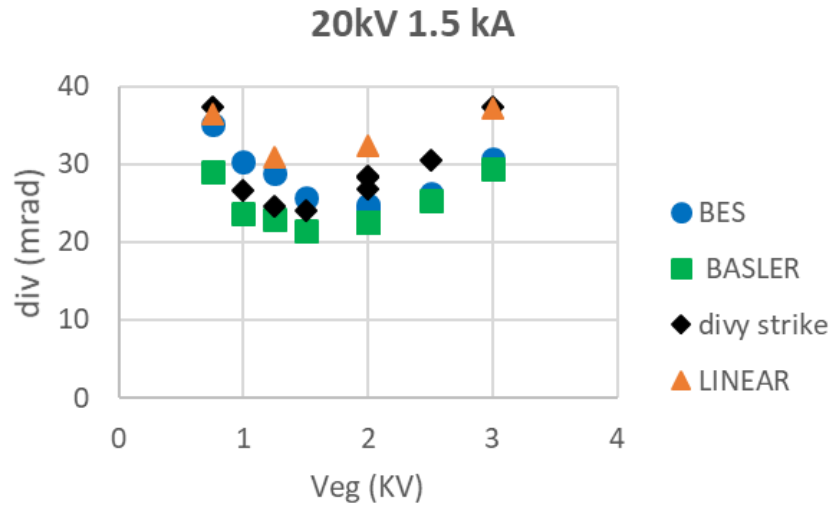
# Characterisation by Beam Emission Spectroscopy

- 6275 20s 1.5/20kV



# Beam physics: comparison of divergence measurements

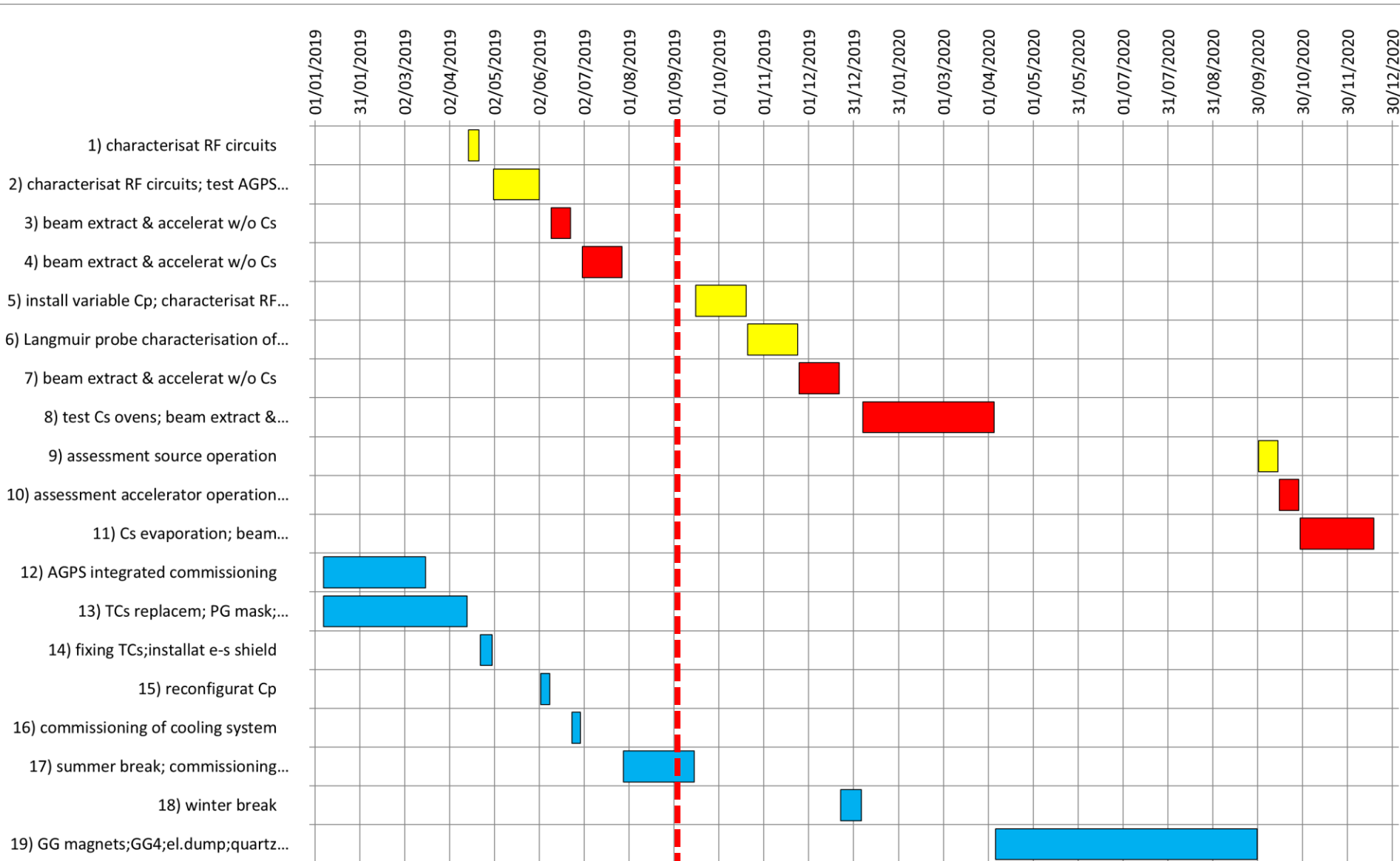
- Values and trends are similar despite different principles of operation



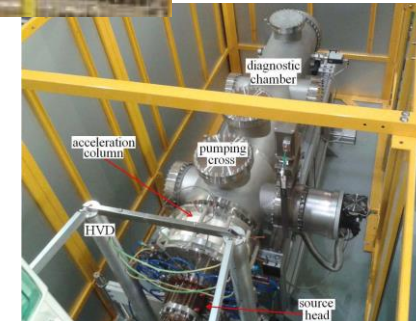
C. Poggi et al., Design and development of an Allison type emittance scanner for the SPIDER ion source, ICIS2019, oral ThuM01  
C. Wimmer et al., Novel comparative measurement of H<sup>-</sup> beam divergences at the BATMAN Upgrade test facility: single beamlet and a group of beamlets, ICIS 2019, poster WedP11



# SPIDER timeline



- High voltage:
  - HVPTF: investigation of voltage holding in vacuum also with B field
  - HVSGTF: High Voltage Short Gap Test Facility
- HVRFTF: investigation of RF voltage holding and of RF circuit developments
- CATS: caesium test stand for investigation of caesium behaviour
- NIO1: small, modular and flexible test facility for test of magnetic and electrostatic configurations of source and accelerator



M. Cavenago et al., Improvements of the NIO1 Installation for Negative Ion Sources, ICIS2019, oral WedA04  
E. Sartori et al., Analysis of current voltage characteristics for Langmuir probes immersed in an ion beam, ICIS2019, poster MonP23  
V. Variale et al., Beam Energy Recovery for Fusion: Collector design for the test on NIO1 source, ICIS2019, poster WedP01  
M. Fadone et al., Interpreting the dynamic equilibrium during evaporation in a Caesium environment, ICIS2019, poster MonP22  
C. Poggi et al., CRISP: a Compact RF Ion Source Prototype for emittance scanner testing, ICIS2019, poster WedP22

- MITICA progressing
  - High voltage insulation tests on-going; breakdown tests due soon
- SPIDER operation without caesium:
  - Negative ion current density up to  $25\text{A/m}^2$
  - Ratio of electron to negative ion current down to 40
  - Beamlet divergence in 20-30mrad range
- From SPIDER to MITICA
  - Improved RF circuits
  - Different configuration of magnetic filter field with no x-point
  - Pumping system expected to be ok
  - Other minor changes to be implemented



प्लाज़्मा अनुसंधान संस्थान  
Institute for Plasma Research



**Thank you for  
your attention**



